



Pauli Kolisoja

MODE 2 RUTTING DESIGN APPROACH

Description of the new ROADEX design approach for Mode 2 rutting on low volume roads

ABSTRACT

The European Union ROADEX Project 1998 – 2012 was a trans-national roads co-operation that aimed at developing ways for interactive and innovative management of low volume roads across the European Northern Periphery. Its main goals were to facilitate co-operation and research into the common problems of constructing and maintaining low volume roads in harsh climates.

Rutting of the road surface due to the development of permanent deformations, both in the road structure itself and in the underlying subgrade, is in most cases the dominant distress mechanism on low volume roads of the Northern Periphery area. From road users' point of view rutting both lowers driving comfort and reduces traffic safety. This is particularly the case when surface water is trapped in ruts, thereby increasing the risk of aquaplaning in summertime and of icing in the wheel path in winter when temperatures fall below 0°C. In addition, rutting can also be very harmful to the structural condition of the road, as it speeds up water infiltration into the road structure, increases the effects of dynamic wheel loads etc.

Rutting can develop in a road for a number of reasons. It may develop in the structural layers due to poor quality material, or as a result of poor drainage making the material more susceptible to permanent deformations. It may also develop in a weak subgrade material if the overall thickness of the structural layers is low. This is a very typical situation on the low volume roads of the Northern Periphery area, particularly during the spring thaw if the subgrade material is frost-susceptible.

This report provides a brief summary on the work done in the ROADEX II project on the classification of rutting phenomena that typically take place on the low volume road networks of the Northern Periphery. It then summarises the design approach developed primarily by the University of Nottingham during the ROADEX III project against Mode 1 rutting, i.e. rutting of the structural layers of low volume road structures. The report then builds on these works and presents a new design approach against Mode 2 rutting, i.e. rutting of the subgrade soil under a LVR having fairly thin structural layers composed of coarse grained aggregate material.

Development of the new design approach is based on the basic ideas put forward earlier during the earlier phases of ROADEX, and extended using advances in technologies now available to ROADEX IV. These enhanced numerical modeling tools have enabled a much more sophisticated and, at the same time, realistic modeling of the mechanical behaviour of the structural system consisting of the aggregate layers and the underlying subgrade soil. In simplified terms the design approach now developed is primarily based on analyzing the load distribution along the aggregate layer so as to assess how wide the area of tyre contact pressure, acting on the road surface, is distributed at the subgrade surface level. After that, a standard geotechnical bearing capacity formula is applied to assess the ultimate load carrying capacity of the subgrade soil, i.e. its ability to resist very rapid accumulation of permanent deformations under a small number of heavy wheel load applications on the road surface.

It is important to note that, at this point, the new design approach is essentially based on back calculating the results of Finite Element modeling in such a way that the same result in terms of ultimate load carrying capacity of the subgrade soil is achieved by a simple hand calculation procedure as would be obtained by making a sophisticated 3D Finite Element modeling of the combination of loading arrangement and road structure system at hand. In future work, however, it would be very important to verify the design approach by full-scale tests performed in-situ and, based on them, make the required refinements into the calculation procedure.

KEYWORDS

Permanent deformation, rutting, subgrade, design, Mode II, low volume road, Northern Periphery

PREFACE

This is a final report from Task D4 of the ROADEX “Implementing Accessibility” project, a technical trans-national cooperation project between The Highland Council, Forestry Commission Scotland and the Western Isles Council from Scotland; The Northern Region of The Norwegian Public Roads Administration; The Northern Region of The Swedish Transport Administration and the Swedish Forest Agency; The Centre of Economic Development, Transport and the Environment of Finland; The Government of Greenland; The Icelandic Road Administration; and The National Roads Authority and The Department of Transport of Ireland.

The lead partner of the ROADEX “Implementing Accessibility” project was The Northern Region of The Swedish Transport Administration and the project consultant was Roadscanners Oy from Finland.

This report summarizes the work done on developing a design approach against Mode 2 rutting, i.e. the development of permanent deformations in the subgrade soil underlying the thin structural layers of a low volume road when the road surface is exposed to wheel loads caused by heavy vehicles.

The report was compiled by Pauli Kolisoja from the Laboratory of Earth and Foundations Structures at the Tampere University of Technology (TUT). Other persons from the TUT team who were involved in the project include Antti Kalliainen, for the Finite Element modeling, and Nuutti Vuorimies, for the supervision and analysis of the triaxial tests performed mainly by laboratory technicians Marko Happonen and Tero Porkka.

Ron Munro from Munroconsult Ltd checked the language of the report. Mika Pyhähuhta of Laboratorio Uleåborg designed the graphic layout.

Finally, last but not least, the authors would like to thank the ROADEX IV Project Steering Committee for their guidance and encouragement during the work

CONTENTS

ABSTRACT	2
PREFACE	3
CONTENTS	4
1. INTRODUCTION	6
1.1 THE ROADDEX PROJECT	6
1.2 D4 “RUTTING, FROM THEORY TO PRACTICE”	7
2. MECHANISTIC DESIGN OF ROAD STRUCTURES	8
3. DEFINITION OF RUTTING MODES	9
4. ROADDEX DESIGN APPROACH ON MODE 1 RUTTING	11
4.1. VARIABLES INCLUDED	11
4.2. BASIC IDEA OF THE MODE 1 DESIGN APPROACH	12
4.3. PRACTICAL APPLICATION OF THE MODE 1 DESIGN APPROACH	13
5. ROADDEX DESIGN APPROACH ON MODE 2 RUTTING	15
5.1. BASIC IDEA OF THE MODELLING APPROACH	15
5.2. INHERENT LIMITATIONS OF THE MULTI-LAYER ELASTIC MODELLING	17
5.3. 3D FINITE ELEMENT MODELLING OF LVR STRUCTURES	18
5.3.1. Principle of the Finite Element model	18
5.3.2. Simulation of the wheel loading	20
5.3.3. Shear strain analysis of some of the modeled structures	21
5.4. VARIABLES INCLUDED INTO THE ANALYSIS	23
5.5. DESCRIPTION OF THE NEW DESIGN APPROACH	24
5.5.1. Basic principle	24
5.5.2. Effect of aggregate and subgrade strength	25
5.5.3. Effect of aggregate layer thickness	27
5.5.4. Effect of wheel configuration	29
5.5.5. Effect of tyre inflation pressure	31
5.5.6. Final outcome of the new design approach development	32
6. DETERMINATION OF THE DESIGN PARAMETERS	37
6.1. DIRECT LABORATORY METHODS	37
6.1.1. Triaxial testing	37

6.1.2. Other laboratory methods	39
6.2. INDIRECT LABORATORY METHODS	40
6.3. SITE INVESTIGATIONS	40
6.3.1. Shear vane test	40
6.3.2. Dynamic Cone Penetrometer, DCP	41
6.3.3. Other sounding methods	42
6.3.4. Falling Weight Deflectometer	42
6.4. SUGGESTED VALUES OF SHEAR STRENGTH PARAMETERS BASED ON ROAD EX RESULTS	43
7. CONCLUSIONS AND RECOMMENDATIONS FOR FUTURE WORK	48
8. REFERENCES	49
APPENDIX	50
APPLICATION EXAMPLES OF THE NEW MODE 2 RUTTING DESIGN APPROACH	50
ANALYSIS OF A BASIC DESIGN CASE	50
EFFECT OF AGGREGATE QUALITY	53
EFFECT OF AGGREGATE MOISTURE CONTENT	55
EFFECT OF SUBGRADE QUALITY	56
EFFECTS OF LOWERING THE DESIGN REQUIREMENTS CONCERNING WHEEL LOAD AND/OR FACTOR OF SAFETY	57

1. INTRODUCTION

1.1 THE ROADEX PROJECT

The ROADEX Project is a technical co-operation between road organisations across northern Europe that aims to share road related information and research between the partners. The project was started in 1998 as a 3 year pilot co-operation between the districts of Finland Lapland, Troms County of Norway, the Northern Region of Sweden and The Highland Council of Scotland and was subsequently followed and extended with a second project, ROADEX II, from 2002 to 2005, a third, ROADEX III from 2006 to 2007 and a fourth, ROADEX “Implementing Accessibility” from 2009 to 2012.



Figure 1-1 The Northern Periphery Area and ROADEX Partners

The Partners in the ROADEX “Implementing Accessibility” project comprised public road administrations and forestry organisations from across the European Northern Periphery. These were The Highland Council, Forestry Commission Scotland and the Western Isles Council from Scotland, The Northern Region of The Norwegian Public Roads Administration, The Northern Region of The Swedish Transport Administration and the Swedish Forest Agency, The Centre of Economic Development, Transport and the Environment of Finland, The Government of Greenland, The Icelandic Road Administration, and The National Roads Authority and The Department of Transport of Ireland.

The aim of the project was to implement the road technologies developed by ROADEX on to the partner road networks to improve operational efficiency and save money. The lead partner for the project was The Swedish Transport Administration and the main project consultant was Roadscanners Oy of Finland. The project was awarded NPP funding in September 2009 and held its first steering Committee meeting in Luleå, November 2009.

A main part of the project was a programme of 23 demonstration projects showcasing the ROADEX methods in the Local Partner areas supported by a new pan-regional “ROADEX Consultancy Service” and “Knowledge Centre”. Three research tasks were also pursued as part of the project: D1 “Climate change and its consequences on the maintenance of low volume roads”, D2 “Road Widening” and D3 “Vibration in vehicles and humans due to road condition”. All of the reports are available on the ROADEX website at www.roadex.org.

1.2 D4 “RUTTING, FROM THEORY TO PRACTICE”

The first aim of Task D4 “Rutting, from theory to practice” was to demonstrate the practical applications of some innovative ROADDEX solutions in the rehabilitation of low volume roads suffering from permanent deformation problems in the Partner areas. The leading idea in the demonstrations was to use ‘fit for purpose’ solutions selected after a sound analysis and understanding of the reasons behind the problems encountered on the individual sites. As the name of task suggests, the main focus was on those problems that appear in the form of permanent deformations, i.e. rutting, which can be the result of different forms of underlying mechanisms. These mechanisms are dealt with in greater detail in a range of ROADDEX reports available on the project website (www.roadex.org). The same website has a number of reports describing in more detail the applications of various types of rehabilitation solutions demonstrated at sites across the low volume road networks of the ROADDEX member countries.

The second main aim of Task D4 was to further develop the analytical design approach against Mode 2 rutting, i.e. the development of excessive permanent deformations in the subgrade soil underlying the relatively thin structural layers of low volume roads. The basic ideas behind Mode 2 rutting design were reported earlier in ROADDEX, but it was not until ROADDEX IV that the available finite element modeling tools enabled a sufficiently realistic modeling of the mechanical behaviour of the structural system, consisting of aggregate layers and underlying subgrade soil, to be effected. This report focuses on describing the development of the new design approach for Mode 2 rutting problems. Some examples of practical applications of the new design approach are also given in the Appendices.

2. MECHANISTIC DESIGN OF ROAD STRUCTURES

The design of low volume roads (LVRs) differs in many respects from that of the more heavily trafficked roads. Because of budgetary constraints, the construction materials of LVRs must in most cases be taken locally from nearby sources, and as a consequence the quality of the materials used may not be the most optimal. For the very same reasons the structural layers of LVRs are in most cases fairly thin, even though it can be well expected that the structures will be exposed at least occasionally to heavy traffic loads induced by transport servicing the local forest industries, aggregate production, farming, fishing etc.

From the mechanistic design point of view there is a fundamental difference between low volume roads and the more heavily trafficked roads. Due to the much weaker structures of LVRs every single heavy load application will bring the structure of a LVR much closer to a structural failure condition than is the case with roads that have higher traffic volumes, and thus also markedly stronger structures. Consequently, deterioration of road structures with heavy traffic volumes normally takes place gradually in the form of a fatigue type of behaviour, while a LVR road may be severely damaged, and actually fail, under a very low number of low repetitions – in the worst extreme case even under a single very heavy vehicle.

Because of the much higher importance of the heavily trafficked road networks it is clear that the vast majority of all the international research work done on developing mechanistic design approaches for road structures has been made with the stronger road structures in mind. The results of this valuable work are abundantly available in the professional literature of highway engineering (e.g. Huag 1993, Ullidtz 1998). The developed deterioration and fatigue models (see Figure 2.1) are, however, unfortunately not directly applicable to LVRs. This is the basic reason why a main effort has been put into the ROADEX project to develop new mechanistic design tools applicable for the design of roads with thin structures resting on fairly weak subgrade materials.

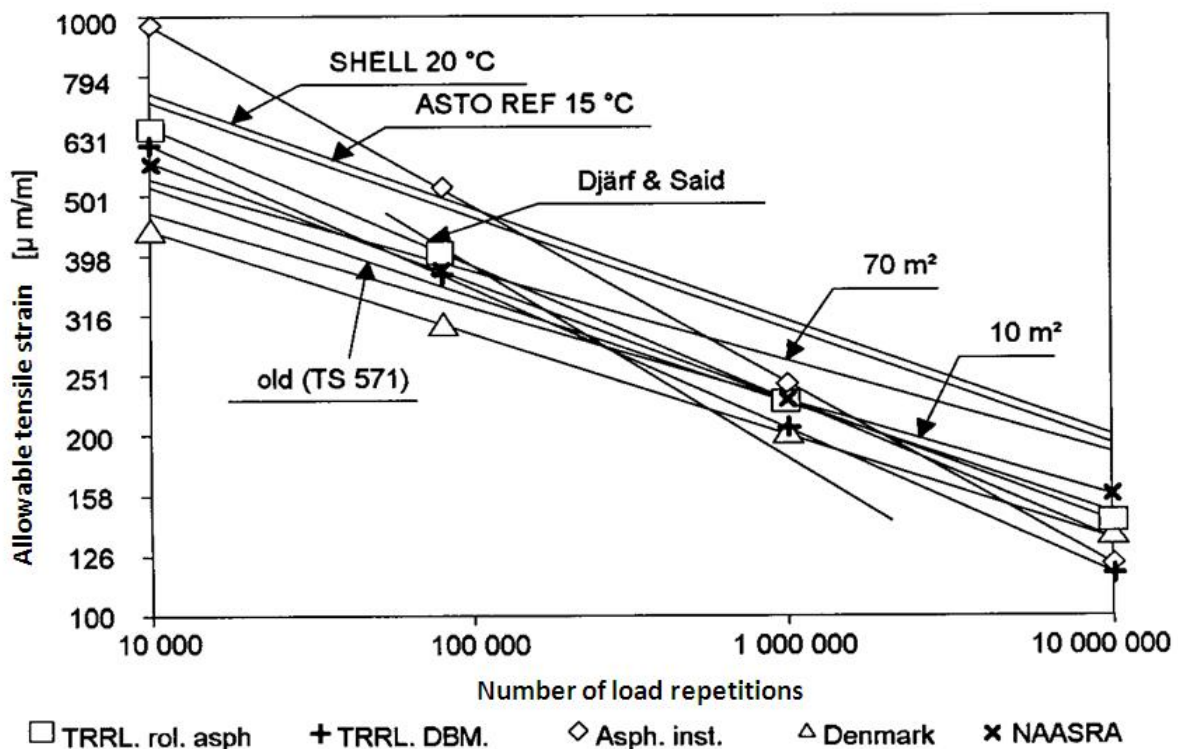


Figure 2.1 Some fatigue models developed for estimating the service life of an asphalt concrete pavement as a function of the tensile strain at the bottom of the pavement under the design wheel load (edited from Ehrola 1996).

3. DEFINITION OF RUTTING MODES

As discussed already above, the visible rutting on a road surface may basically result from a number of different phenomena taking place under the surface. However, when thinking about what types of maintenance and rehabilitation measures could be taken it is of the utmost importance to identify the correct mechanisms behind the rut development. For this reason a new definition of rutting modes was suggested in the ROADDEX II project by Dawson and Kolisoja (2004).

According to the suggested classification of rutting modes the development of cross sectional unevenness of a road surface may be result from four different fundamental mechanisms that are called Mode 0, Mode 1, Mode 2 and Mode 3, respectively. A brief description of each of the rutting modes is given in the paragraphs following. For a more complete description of the Modes reference should be made to the earlier ROADDEX reports (Dawson & Kolisoja 2004 and Dawson et al. 2008), and the eLearning material available at the ROADDEX website (www.roadex.org).

Mode 0

Compaction of the non-saturated aggregate materials in the structural layers of a road is called Mode 0 rutting (Figure 3.1). Especially in the case of gravel roads this type of rutting phenomenon is, however, not very harmful because it is self-stabilizing – i.e. compaction under trafficking hinders further compaction.

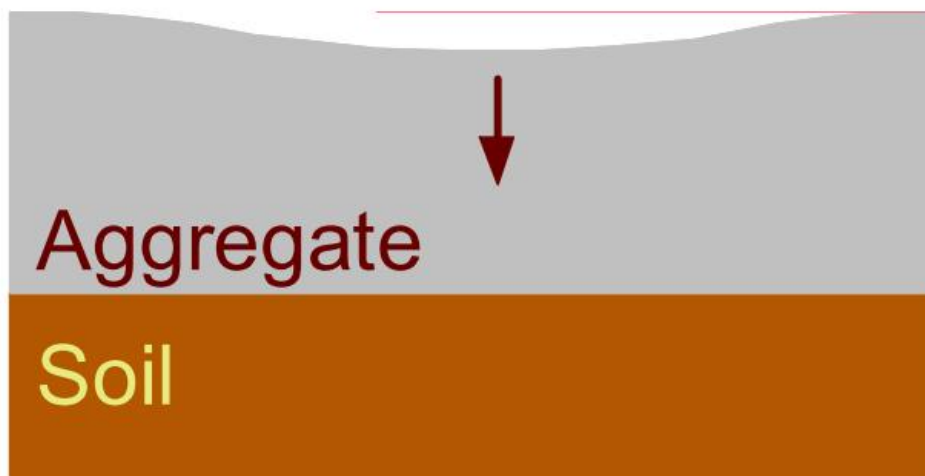


Figure 3.1 Mode 0 rutting – compaction of the granular layers alone (Dawson & Kolisoja 2004).

Mode 1

In weaker granular materials local shear strain close to the wheel loading may occur. This gives rise to dilative heave immediately adjacent to the wheel track (Figure 3.2) in which large plastic shear strains and consequent dilation takes place, leading also to loosening of the base course material. This type of rutting is thus primarily a consequence of inadequate granular material shear strength in the aggregate relatively close to the pavement surface.

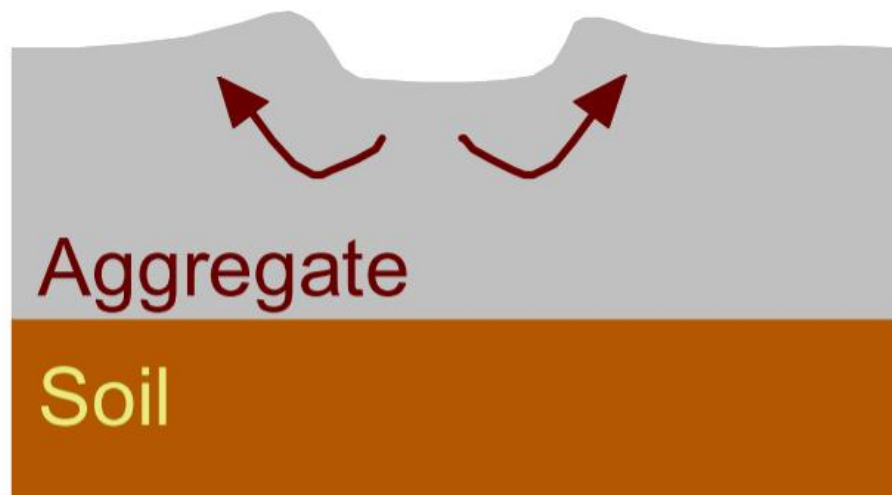


Figure 3.2 Mode 1 rutting – shear deformation within the granular layers of the pavement, near to the surface (Dawson & Kolisoja 2004).

Mode 2

When the aggregate quality is better, then the pavement as a whole may rut. Idealized, this can be viewed as the subgrade deforming, and the granular layer(s) deflecting bodily on it (Figure 3.3). The surface pattern is of a broad rut with possibly slight heave remote from the wheel path.

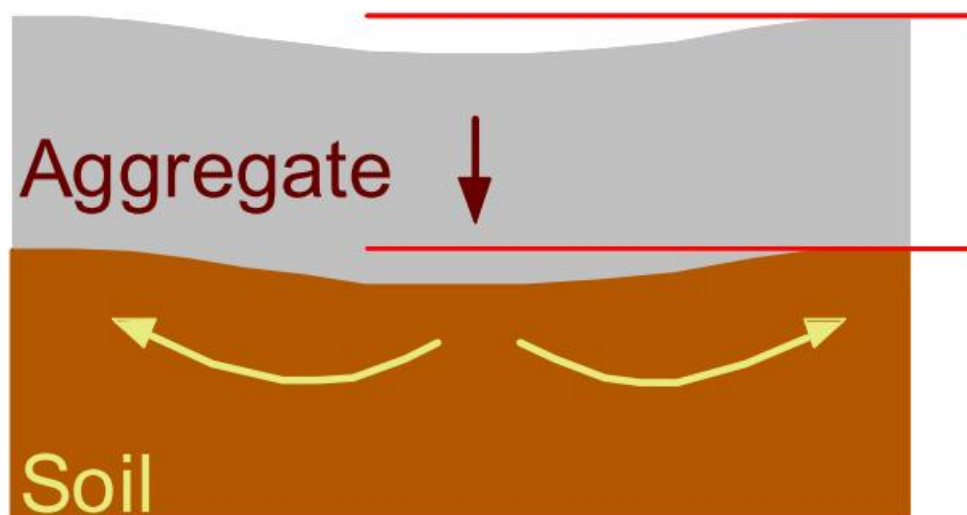


Figure 3.3 Mode 2 rutting – shear deformation within the subgrade with the granular layer following the subgrade (Dawson & Kolisoja 2004).

Mode 3

Rutting may also be due to the surface wear of the pavement structure caused, for example, by studded tyres. This type of rutting can, however, not be considered as a structural problem of the road and is therefore not discussed in any greater detail in this context.

4. ROADEX DESIGN APPROACH ON MODE 1 RUTTING

4.1. VARIABLES INCLUDED

A new type of mechanistic design approach against Mode 1 rutting was developed as part of the ROADEX III project by the University of Nottingham (Dawson et al. 2007, Dawson et al. 2008, Brito et al. 2009). Their approach is based on analyzing the shear stresses experienced at various points in a road structure exposed to a wheel loading, and comparing these stresses with the shear strength of the aggregate material involved. The design approach included the following variables:

- Wheel configuration: dual wheel/super single
- Tyre inflation pressure: 800 kPa/400 kPa
- Thickness of the granular layer
- Aggregate stiffness/subgrade stiffness ratio
- Mechanical properties of the unbound (base course) aggregate

Wheel configuration and tyre inflation pressure

In the analytical calculations forming the base of the design approach, the loading arrangement of the wheel was assumed to be either a super-single tyre loading, or a pair of dual tyres. The tyre inflation pressures considered in the analysis were 800 kPa, and 400 kPa, respectively. Assuming that the contact area between the tyres and the road surface was circular, the loadings of the respective tyre arrangements were as indicated in Figure 4.1.

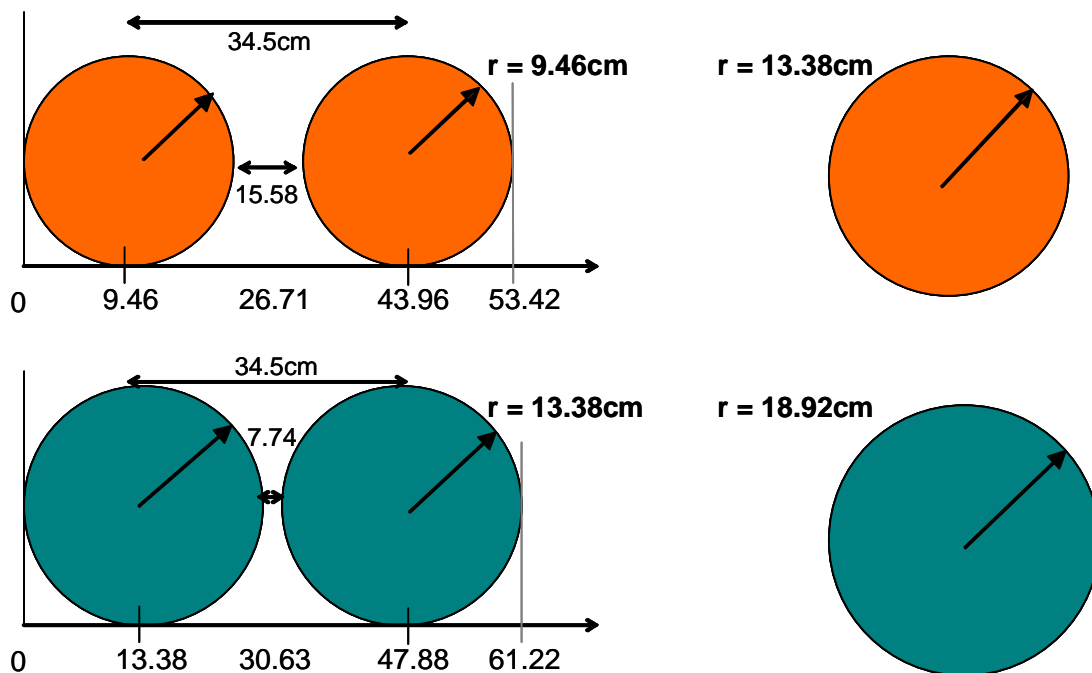


Figure 4.1 The assumed equivalent, circular loaded areas to simulate dual and super-single tyres. Top at 800 kPa and bottom at 400 kPa. (Dawson et al. 2007).

Thickness of the granular layer(s)

In the developed Mode 1 design approach, the total thickness of the unbound aggregate layer(s) is expressed in relative terms, i.e. in relation to the radius of the loaded area under one tyre. The calculations included altogether five different aggregate thickness / loaded area ratios, varying from 1.0 to 3.5. Depending on the wheel configuration and tyre inflation pressure being considered this corresponded to an aggregate layer thicknesses varying from 135 mm to 665 mm.

Aggregate stiffness/subgrade stiffness ratio

The difference between the stiffnesses of the aggregate material and the underlying subgrade was also taken into account in relative terms. In the calculations the lowest value of this ratio was 2 while the highest value was 8.

Mechanical properties of the aggregate material

The stiffness properties of the unbound aggregate material were derived from an existing data base of earlier test results available at the University of Nottingham. After initially performing calculations with parameter values corresponding to three different actual aggregate materials it was discovered that the results obtained were not very sensitive to the differences in the non-linear stiffnesses of the aggregate material.

The shear strength of the aggregate material was assumed to follow the Mohr-Coulomb failure criterion. Consequently, the strength parameters cohesion “c” and friction angle “ ϕ ” were used to describe the strength of the unbound aggregate material, as explained in more detail in the following chapter.

4.2. BASIC IDEA OF THE MODE 1 DESIGN APPROACH

The design approach developed against Mode 1 rutting is based on a so called ‘proximity to failure analysis’. That is to say that the stresses experienced at different points of the pavement structure, as represented by the loci of maximum stress points (the blue and brown lines for the examples of dual and super-single tyre configurations in Figure 4.2, respectively), are compared to the ultimate shear strength of the unbound aggregate material as indicated by the red dotted line in the pq stress space of Figure 4.2.

To enable the ultimate shear strength of the aggregate to be compared with the stresses incurred in the pavement structure a somewhat arbitrary line connecting the point 250 kPa at the horizontal p-axis and 250 kPa at the vertical q-axis was defined. Along this line, the distance from the horizontal axis to the failure line, S, is compared to the distance of the actual locus of maximum shear stresses, e.g. S for super single and S_{dt} for dual tyres in Figure 4.2.

The stress calculations used in developing the design approach were performed using a multi-layer non-linear elastic software KENLAYER (Huang 1993). Due to the inherent limitations of the applied modeling tool the stresses in some of the calculation points were considered unrealistic and thus omitted from further analysis, as explained in more detail in the actual research report by Dawson et al. (2007).

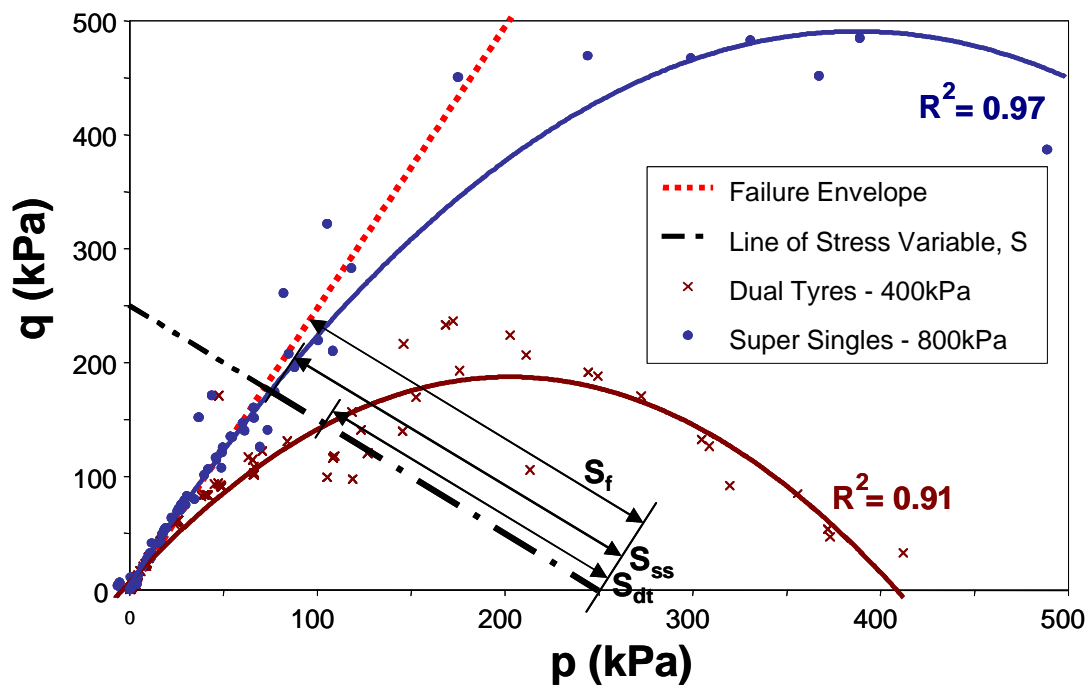


Figure 4.2 Principle of the 'proximity to failure approach' (Dawson et al. 2007).

4.3. PRACTICAL APPLICATION OF THE MODE 1 DESIGN APPROACH

Because it is not realistic to assume that local road engineers working case by case with real LVRs will have access to very sophisticated calculation tools and methods, a fair amount of effort in the ROADDEX project was focused on developing an easy-to-use interface to the modeling approach. In practice this meant a set of tabulated S-values for different combinations of the variables involved (Dawson et al. 2007). The value of S obtained can then be compared to the value of S_f calculated based on the assumed values of shear strength parameters of the unbound aggregate. According to the suggestion made by Dawson et al. (2007) this relationship should not exceed 0.90 in normal drainage conditions, and 0.75 in wet or thawing conditions.

An even more user-friendly practical application of the Mode 1 rutting approach is available in a software tool developed by Roadscanners Ltd on the ROADDEX website (www.roadex.org). The tool enables the user to define the loading arrangement, aggregate layer thickness and the material parameters just by means of simple choices and input values (Figure 4.3).

The selection of shear strength parameters for various types of aggregate materials that can be applied in the structural analysis of low volume roads is discussed in Chapter 6 of this report.

Step 1 : Structure and loading

Properties of traffic and structure

Tyre settings

☒ Dual

Pressure

☐ 400 kPa

☒ 800 kPa

Initial parameters

Wheel load (kN)	50
Tyre contact area (m ²)	0,03
Radius (mm)	99,74
Aggr. thickness ratio	5,01

Properties of base course material

Aggregate setup

Thickness (mm)	500	Ebas / Esub
Base course moduli (Eb)	200	
Subbase moduli (Esub)	30	
		6,66667

Material quality

☒ Good

☐ Medium

☐ Poor

Moisture content

☒ Normal

☐ Saturated

Compaction level

☒ Appropriate

☐ Inappropriate

Fill	Cohesion
50	25

Step 2 : Rounding

Confirm used values

Aggregates thickness / Radius	3.5
Ebas / Esub	8

Calc. rounded values

Step 3 : Result

Calculation

☐ Use exact value (interpolate)

☒ Aggregate thickness / Radius ratio

☐ Ebas / Esub ratio

S (kPa)	222,6
Sf (kPa)	257,9

Risk after heavy rains

90% of Sf (kPa)	232,1
Result (is S < 90% Sf)	OK

Calculate

Figure 4.3 A view of the ROADEx software tool tailored for practical applications of the Mode 1 rutting design approach (www.roadex.org).

5. ROADEX DESIGN APPROACH ON MODE 2 RUTTING

Some early attempts of developing a mechanistic (or 'geotechnical') design approach for Mode 2 rutting were also made during the ROADEX II and ROADEX III projects (Dawson & Kolisoja 2004 and Dawson et al. 2007). These attempts were, however, inconclusive mainly due to the limitations of the available modeling tools in modeling the complex mechanical behaviour of unbound granular materials. Recently however, this limitation has, markedly eased up and at present some relatively easy-to-use software packages enable realistic modeling of the mechanical responses of LVR structures exposed to wheel loads. A new type of design approach against Mode 2 rutting developed based on 3D Finite Element modeling accomplished using the software tool PLAXIS is described herein.

5.1. BASIC IDEA OF THE MODELLING APPROACH

The development of the new design approach against Mode 2 rutting had the following assumptions as its starting point:

- The structure to be designed is so weak that it has a risk of rapid deterioration even under a relatively low number of load repetitions, i.e. the margin of safety against an immediate full failure is not high. Therefore, a geotechnically based approach in the design is required.
- The assumption above means in practice that the structural layers of the road comprising coarse grained aggregates are relatively thin, of the order of half a metre at maximum.
- The underlying subgrade material is a soft silt or clay type of material, or a moraine type of material in a thawing condition. (On a more coarse grained subgrade material in good drainage conditions the probability of a rapid Mode 2 type of rut development should be very low.)
- The load duration time of moving wheels is low. Consequently the strength properties of the fine grained subgrade under a short term loading can be described using the undrained shear strength of the subgrade material.

With these assumptions in mind the developed design approach makes use of a standard geotechnical bearing capacity formula to assess the ultimate load that can be applied on the surface of a soil layer before it fails / collapses (Figure 5.1). The key questions remaining after this assumption are:

1. how is the wheel load distributed as it is transferred along the structural layers resting on top of the subgrade material, and
2. what is the undrained shear strength of the subgrade material.

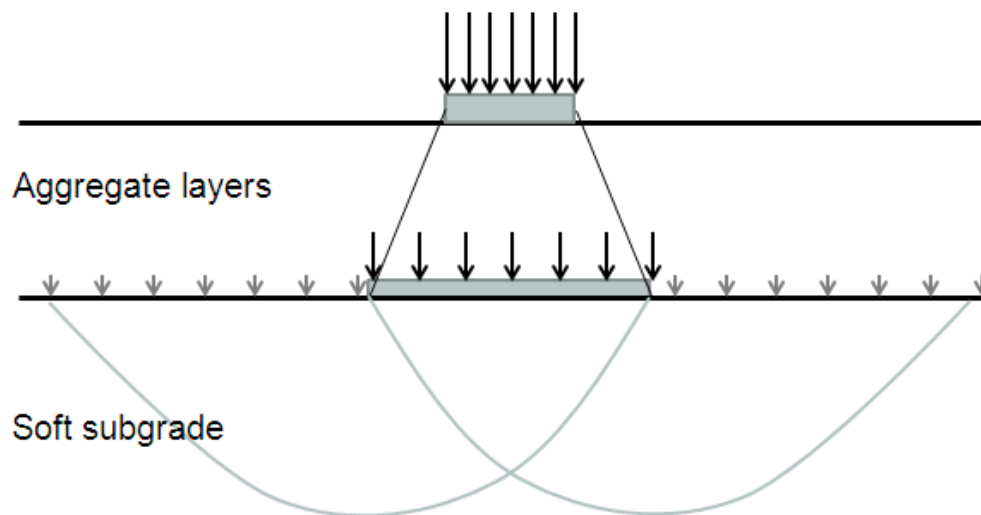


Figure 5.1 Basic idea of the new design approach against Mode 2 rutting.

Case by case assessments of the subgrade shear strength must inevitably be based on normal geotechnical site and laboratory investigation methods, and the practical experimental knowledge built on them. At the same time, the load distribution at the subgrade surface level is clearly an issue deserving a closer consideration.

For instance, in normal consolidation settlement calculations the load distribution is very often assumed to follow the simple model of a '1:2 distribution' as shown in Figure 5.2. In the case of a 50 kN wheel load acting on top of a LVR structure consisting of 0.4 m of aggregate layers this assumption would predict an increase of 136 kPa in the vertical stress at subgrade level. Note however, that this prediction does not by any means take into account the type of material in between the road surface and the subgrade level, nor the properties of the subgrade material itself. The prediction model would also follow the same rule whatever is the thickness of the aggregate layer. Because these limitations can in many respects be considered as contradictory to a common sense engineering judgement, it is quite clear that this is an issue deserving a closer attention and analysis before that basic idea of the design approach can be applied further.

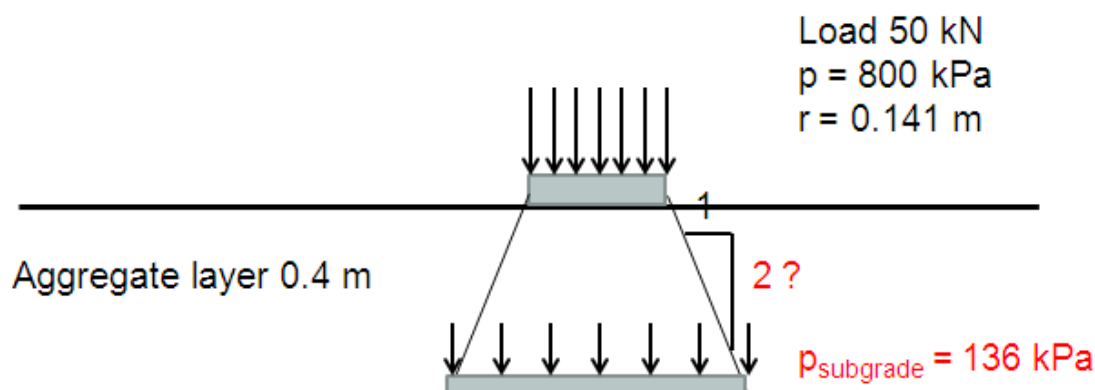


Figure 5.2 Assessment of the vertical stresses according to the so called '1:2 distribution' model.

5.2. INHERENT LIMITATIONS OF THE MULTI-LAYER ELASTIC MODELLING

A logical step to be taken in a more detailed analysis of the problem described above would be to use a multi-layer linear or non-linear elastic modeling approach generally applied in the stress-strain distribution analyses of pavement structures. If the same type of wheel loading and layer thickness as shown in Figure 5.2 are used, and the assumptions concerning the stiffness properties of subgrade and aggregate layer are as indicated in Figure 5.3, a multi-layer linear elastic analysis predicts a maximum value of vertical stress increase of 69 kPa directly beneath the centre of the loaded area. This is a value that is clearly much lower than that obtained with a '1:2 distribution' model.

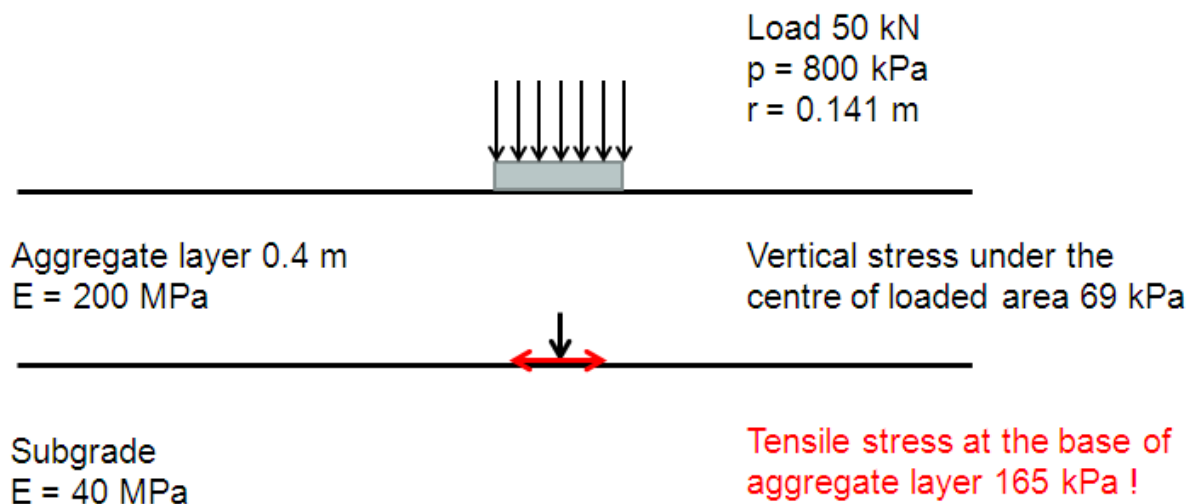


Figure 5.3 An example of multi-layer linear elastic modeling of a low volume road structure.

An even more striking observation in these results is, however, that the tensile stresses at the bottom of the unbound layer, directly beneath the loaded area, can be as high as 165 kPa. For an unbound material essentially incapable of taking tensile stresses this is of course an unrealistic situation that certainly can be assumed to have an effect also on the distribution of vertical stresses.

The phenomenon is even more pronounced if the subgrade underlying the aggregate layer is softer than that assumed in Figure 5.3. For subgrade stiffness values of 20 MPa and 10 MPa the maximum values of tensile stresses at the base of the aggregate layer are 242 kPa and 314 kPa, respectively. At the same time, the corresponding predicted values of vertical stress increase, due to the wheel loading directly beneath the centre of the loaded area, are 47 kPa and 31 kPa, thus predicting that the softer the subgrade material is, the lower are the stresses it is exposed to.

The simple and obvious explanation for the results described above is that in the linear elastic modeling approach the layer materials are intrinsically assumed to have an unlimited capacity to resist tension, which in the case of unbound materials is of course a totally wrong assumption.

Another important built-in limitation in practically all of the multi-layer linear and non-linear modeling approaches is that each of the structural layers in the calculation model is assumed to have a constant stiffness throughout the layer. However, as the resilient deformation properties (i.e. the stiffness) of unbound granular materials are well known to be highly stress-dependent, the stiffness of the layer material in reality changes markedly also in the horizontal direction, with stresses obviously much higher below the loaded area than alongside it. Also this limitation can be assumed to have a distinct effect on the results obtained if the prediction of the vertical stress distribution is based on the multi-layer modeling approach.

5.3. 3D FINITE ELEMENT MODELLING OF LVR STRUCTURES

5.3.1. Principle of the Finite Element model

In the recent years the rapid development of computer technology and available calculation software tools have opened totally new windows for the modeling of the types of pavement structures typically found on low volume roads. In this research the applied software tool has been the 3D Finite Element modeling code “PLAXIS” from the Netherlands. In comparison to the multi-layer linear elastic modeling it enables a much more realistic calculation model to be built both with regard to the model geometry and the mechanical properties of the aggregate materials, and any soil layers within it. The type of FE model used for single wheel load configuration in this research is shown in Figure 5.4. Corresponding variations of the model were also created for the dual wheel configuration, lowered tyre inflation pressure and different thicknesses of the structural layers.

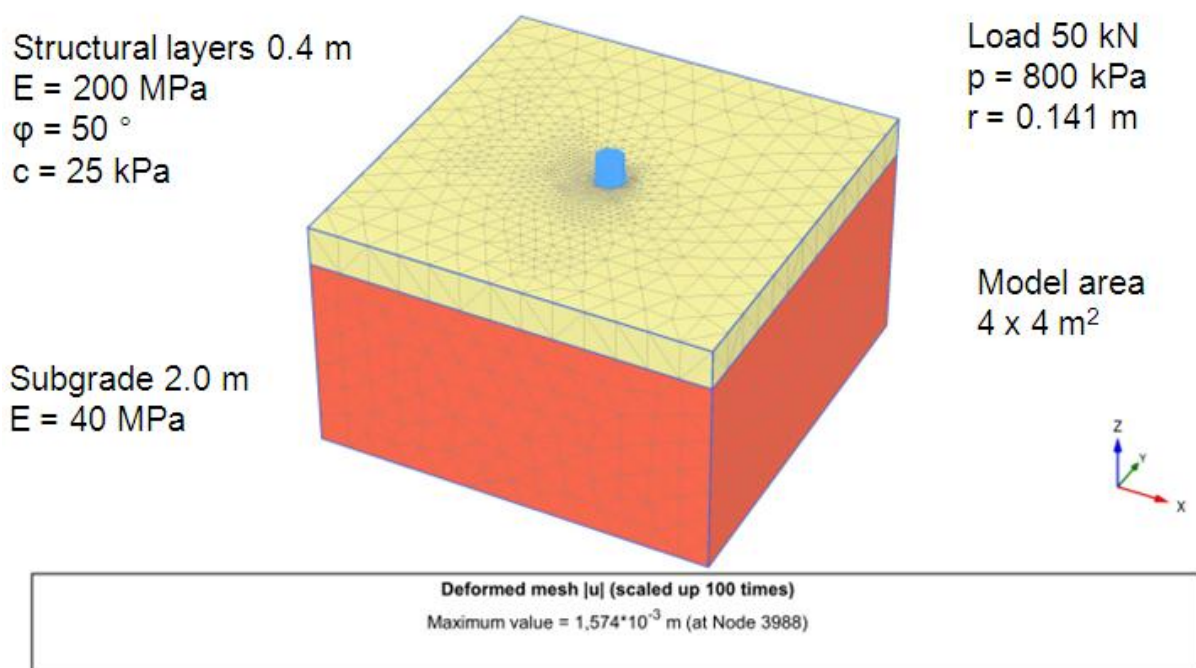


Figure 5.4 The principle of 3D Finite Element model used in this research to represent the single wheel load configuration resting on top of a 0.4 m thick LVR structure.

The material model employed in FE modeling is the Mohr-Coulomb model in drained conditions for the aggregate layer, and in undrained conditions for the subgrade soil. The undrained shear strength of the subgrade was assumed to increase by 1.5 kPa per metre of depth from the initial values at the top the subgrade. A more detailed description of the material model can be found in the user's manual set of the PLAXIS software package.

Table 5.1 gives a summary of the actual values of the material parameters used in the present FE modeling analyses.

Table 5.1 A summary of the material parameter values employed in the FE analyses.

Subgrade quality	γ_{unsat} kN/m ³	γ_{sat} kN/m ³	e_{init}	E' MPa	ν	$S_{u,ref}$ kPa	$S_{u,inc}$ kPa/m
Weak	18	18	0.5	10	0.4	10	1.5
Semi-weak	18	18	0.5	15	0.4	15	1.5
Medium	18	18	0.5	20	0.4	20	1.5

Aggregate quality	γ_{unsat} kN/m ³	γ_{sat} kN/m ³	e_{init}	E' MPa	ν	c'_{ref} kPa	ϕ °	ψ °
Poor	21	22	0.3	150	0.3	3	40	5
Medium	21	22	0.3	150	0.3	10	45	5
Good	21	22	0.3	150	0.3	25	50	5

The key difference in the model used compared a multi-layer linear elastic model is that it enables a realistic simulation of the limited strength of the available materials to be made. Thus it provides a much more plausible picture of the distribution of stresses and strains within the model to be obtained than is the case with the more robust modeling approaches. As an example, the distribution of the vertical stresses at the subgrade surface level under the loading condition set out in Figure 5.4 are shown as plane and cross sectional views in Figures 5.5 and 5.6, respectively.

According to this model the maximum values of vertical stress at the subgrade surface are above 80 kPa near to the centre of the loaded area. A very important message however from both figures is that the distribution of the vertical stress increase at the subgrade surface level due to the 50 kN wheel loading is far from the rectangular shape as predicted by the simple '1:2 distribution' model of Figure 5.2. So the question remains, if the modeled behaviour should be simplified in the form of rectangle indicated by the green dotted line, yellow dotted line, or maybe something in between the two, in Figure 5.6 to make it applicable for the subgrade ultimate bearing capacity prediction of the type outlined in Figure 5.1.

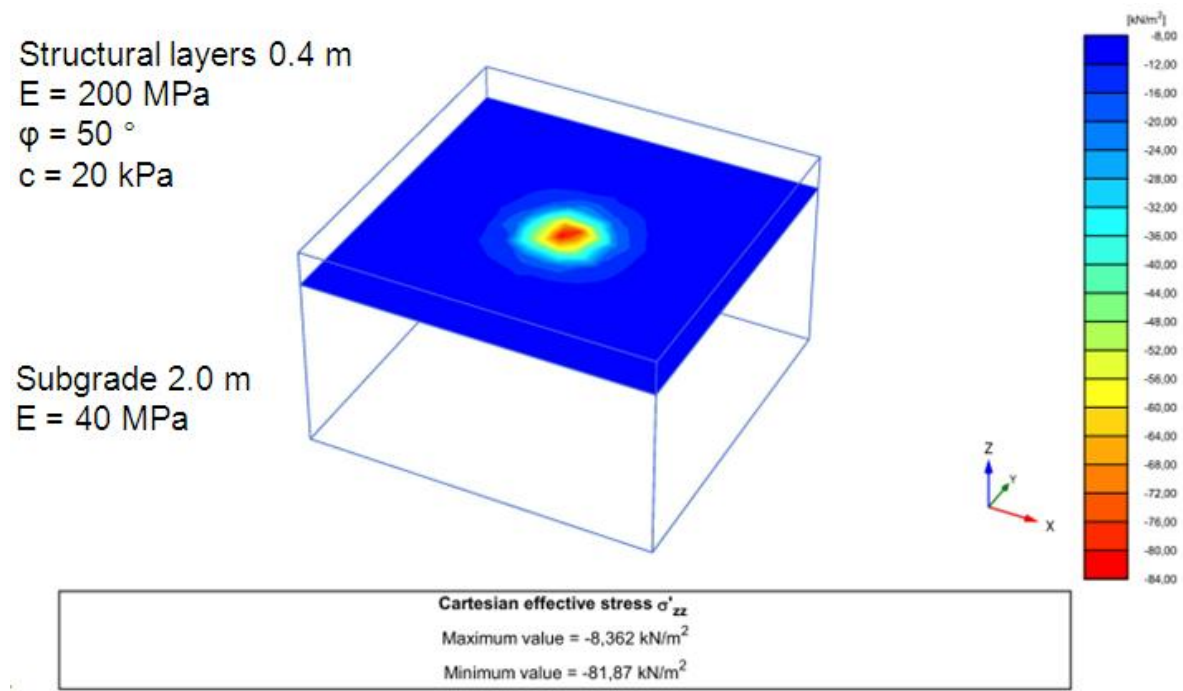


Figure 5.5 Distribution of vertical stresses in a plane located at the subgrade surface of the model shown in Figure 5.4.

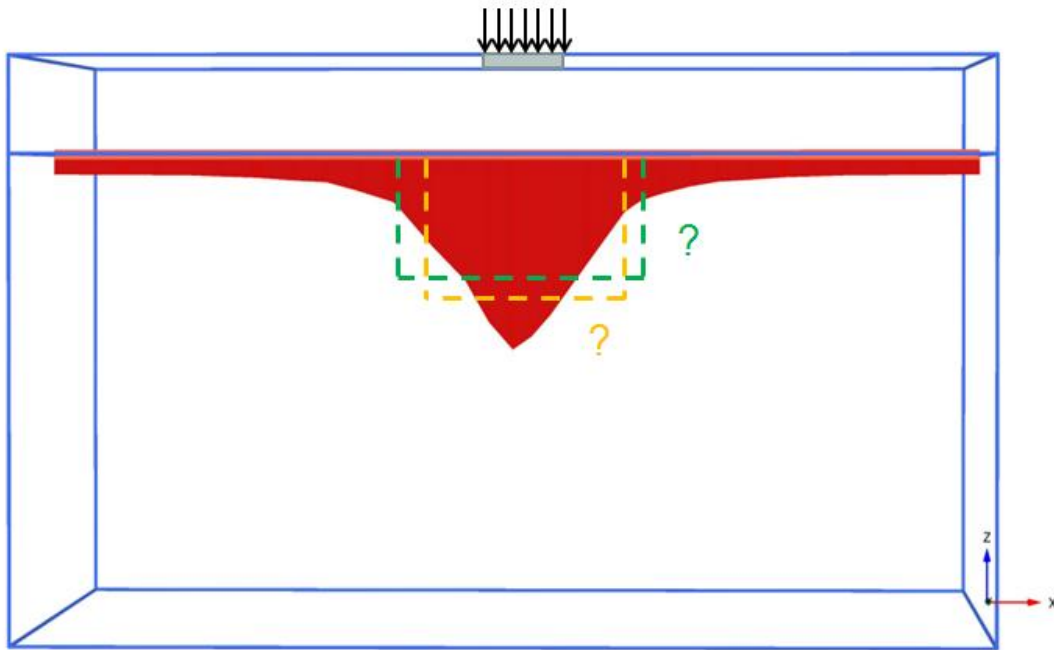


Figure 5.6 Distribution of vertical stresses at the subgrade surface level in a cross sectional view along a plane symmetrical to the centre of the loaded area of the model shown in Figure 5.4.

5.3.2. Simulation of the wheel loading

For the FE analyses, the wheel load was applied incrementally in the model in steps of 10 kN for each of the different combinations of wheel configuration, material properties and aggregate layer thickness. After each load increment the applied software tool solved the equilibrium condition of the model before the next load increment was added. As a result, the predictions for the deflections of the road surface as a function of the wheel load were output in the form of the four different combinations of aggregate and subgrade types shown in Figure 5.7. The respective material properties corresponding to each of these loading simulations are presented in more detail in the following sections.

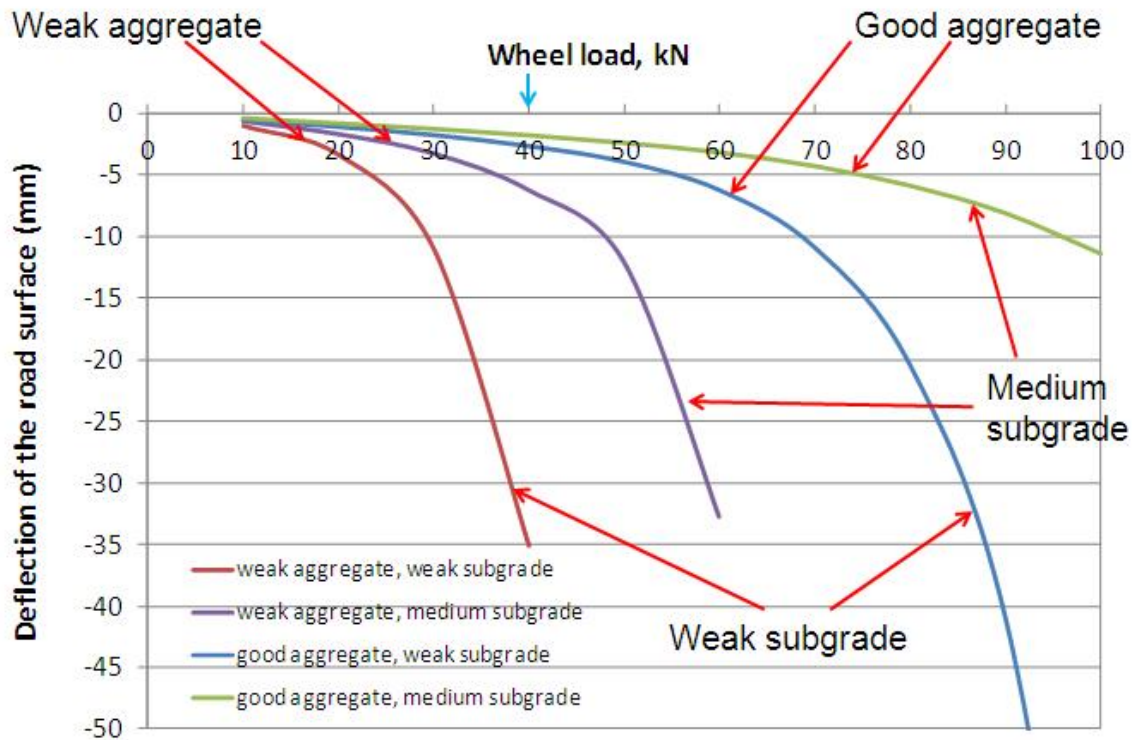


Figure 5.7 Some examples of predicted deflections of the road surface as a function of the wheel load obtained using the type of model shown in Figure 5.4.

Figure 5.7 indicates clearly that the predicted ultimate bearing capacity of the subgrade (essentially its capacity to resist Mode 2 type of rutting), in extreme loading conditions depends not only on the type of subgrade material but also quite markedly on the properties of the material above it. In practical terms, from the subgrade point of view, a good quality material is able to distribute the wheel load acting on the road surface much more efficiently than a poor quality weak aggregate. A good quality subgrade thus provides a better performance for the whole structural system. If however the simple '1:2 distribution' model had been used to predict load spreading, no distinction could have been made between the good and the weak aggregate. The same holds true also for the linear elastic modeling, provided that the **stiffness values** of the good and weak aggregate are assumed to be the same.

One limitation to be acknowledged in the type of modeling approach described above is that the model geometry remains the same throughout the loading simulation. In comparison to the respective real loading conditions, the principal difference is that the contact area between road surface and tyre does not change, but the contact pressure does. Under an actual vehicle tyre the situation would be reversed, i.e. the contact pressure would remain basically the same, close to the tyre inflation pressure, whilst the contact area would increase relative to the wheel load. This limitation is, however, not considered very important because at the load level of 50 kN (and tyre inflation pressure of 800 kPa), i.e. the most likely critical level of wheel loading in practice, the difference dies out.

5.3.3. Shear strain analysis of some of the modeled structures

Figure 5.8 gives an example of the different types of more detailed analyses for which the FE modeling can be used in the effort to develop a better understanding of the mechanical behaviour of low volume road structures. The figure presents shear strain distributions in each of the loading simulations shown in Figure 5.7 at a moment when the wheel load has reached the level of 40 kN.

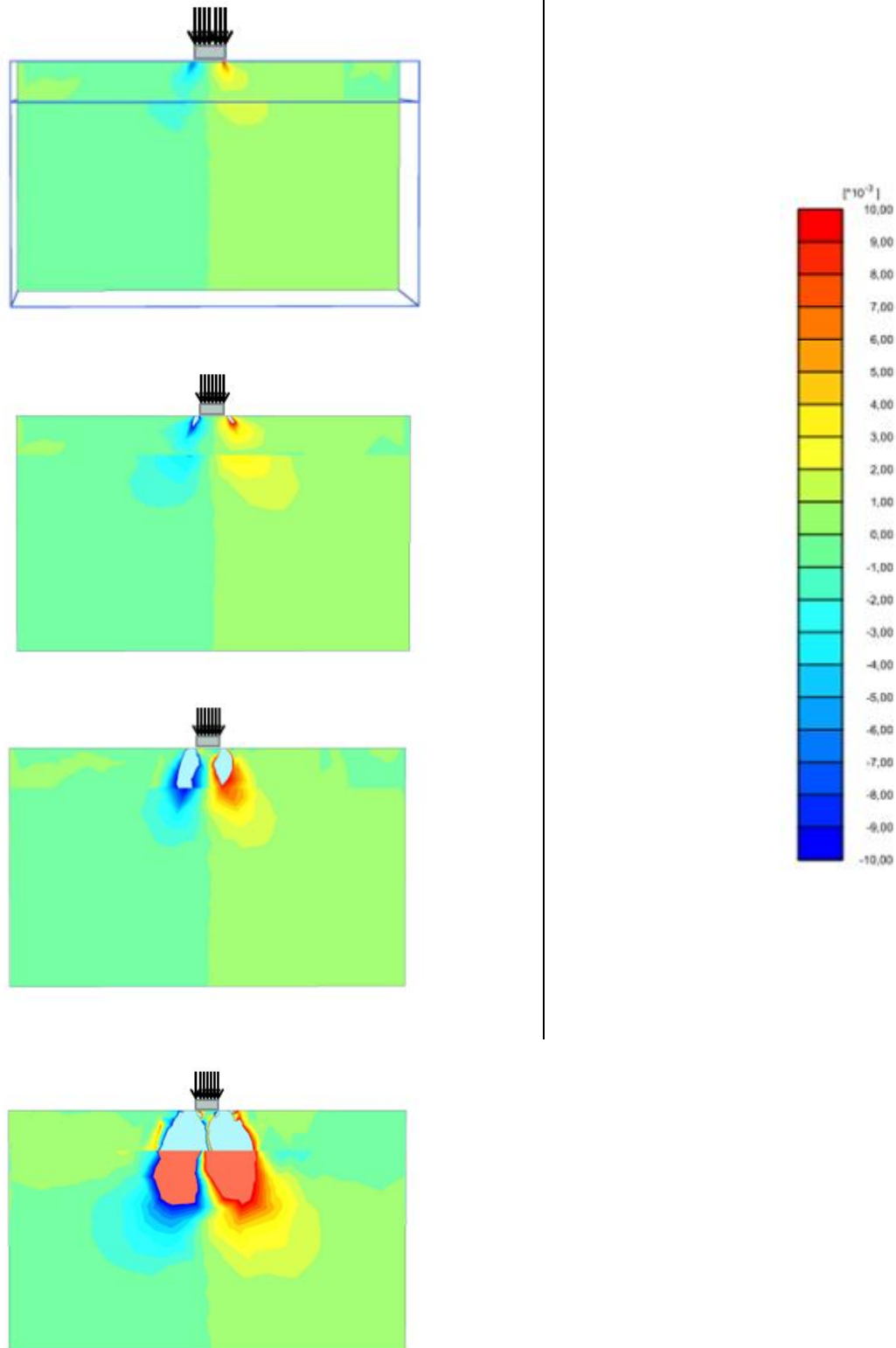


Figure 5.8 Shear strain distributions in the loading simulations of Figure 5.7 when the wheel load is 40 kN. The light blue areas in the two lowermost diagrams represent values beyond the scale i.e. exceeding 1 % ($10 \cdot 10^{-3}$).

The top diagram of Figure 5.8 presents the shear strain distribution in a structure made of good quality aggregate that is resting on a medium quality subgrade (details behind these definitions will be explained later). Here we can see that the shear strains reach or exceed a level of 5×10^{-3} , i.e. 0.5 %, only within a very limited part of the structure next to the edges of the loaded area. At the

same time, the mobilized level of shear strains remains fairly low in the other parts of the aggregate layer and also throughout the subgrade. From the respective load-deflection curve shown by the green line in Figure 5.7, we can see that the wheel load of 40 kN is in this case clearly far from its ultimate value.

The second diagram from the top in Figure 5.8 shows the same good quality aggregate resting on a weak subgrade material. It still provides good enough load spreading to protect the subgrade from the mobilization of excessive shear strains. However, when the aggregate is changed to poor quality (the two lower diagrams in Figure 5.8), it is quite obvious that the wheel load is punching much more directly through the aggregate layer, and thus also mobilizing much higher shear strains into the subgrade material. In the particular case of the combination of weak aggregate and weak subgrade the wheel load of 40 kN is actually already creating a failure condition represented by the very large surface deflection exceeding 30 mm (indicated by the brown curve in Figure 5.7).

5.4. VARIABLES INCLUDED INTO THE ANALYSIS

In the same way as was the case with Mode 1 rutting discussed in Chapter 4 it is obvious that the overall performance of the structural system shown in Figure 5.1 depends on a number of variables. In this research the focus has been on the following factors considered to be the most important:

- Wheel configuration; dual wheel or super single
- Tyre inflation pressure
- Thickness of the aggregate layer
- Effective strength parameters of the aggregate material; in practice, the friction angle and (apparent) cohesion
- Undrained shear strength of the subgrade material

A summary of the variables and respective parameter values included in the analyses is presented in Table 5.2.

Among the factors that can be assumed to have at least some influence on the results of analyses such as those shown above are the relationships between the strength and stiffness properties of the aggregate and the subgrade materials. Within the practical limitations of this project it was not, however, possible to make any detailed sensitivity analysis on the effect of these factors. The variables that were given constant values in the analyses included:

- Stiffness of the aggregate layer, 150 MPa
- Stiffness of the subgrade material, 20 MPa, 15 MPa or 10 MPa depending on the undrained shear strength of the subgrade material 20 kPa, 15 kPa or 10 kPa, respectively.
- Radius of the circular contact area between the tyre and road surface, 0.141 m, except in the case of dual wheels with tyre inflation pressure of 800 kPa when it was given the value 0.100 m for both of the dual tyres.

Table 5.2 A summary of the variables included in the FE analyses performed in the project.

Wheel configuration	Tyre inflation pressure	Aggregate layer thickness	Friction angle φ	Apparent cohesion, c	Subgrade shear strength
Single	800	0.4	50	25	20
Single	800	0.4	50	25	15
Single	800	0.4	50	25	10
Single	800	0.4	45	10	20
Single	800	0.4	45	10	15
Single	800	0.4	45	10	10
Single	800	0.4	40	3	20
Single	800	0.4	40	3	10
Single	800	0.3	50	25	15
Single	800	0.3	50	25	10
Single	800	0.3	45	10	15
Single	800	0.3	45	10	10
Single	800	0.5	50	25	15
Single	800	0.5	50	25	10
Single	800	0.5	45	10	15
Single	800	0.5	45	10	10
Dual	800	0.4	50	25	15
Dual	800	0.4	50	25	10
Dual	800	0.4	45	10	15
Dual	800	0.4	45	10	10
Dual	800	0.4	40	3	20
Dual	800	0.4	40	3	15
Dual	800	0.4	40	3	10
Dual	400	0.4	50	25	15
Dual	400	0.4	50	25	10
Dual	400	0.4	45	10	15
Dual	400	0.4	45	10	10
Dual	400	0.4	40	3	20
Dual	400	0.4	40	3	15
Dual	400	0.4	40	3	10

5.5. DESCRIPTION OF THE NEW DESIGN APPROACH

5.5.1. Basic principle

As concluded already in chapter 5.1 it is necessary to have a realistic estimate of the wheel load distribution along the aggregate layer before a geotechnical bearing capacity equation approach can be carried out for the assessment of the ultimate load carrying capacity of a subgrade, i.e. its ability to resist rapid accumulation of Mode 2 rutting in extreme loading conditions. For this it is necessary to define a quantity that will be called a “load distribution factor” (LDF). When defined as shown in Figure 5.9 the LDF will have a larger numerical value when the aggregate layer is more able to efficiently spread the load, and vice versa.

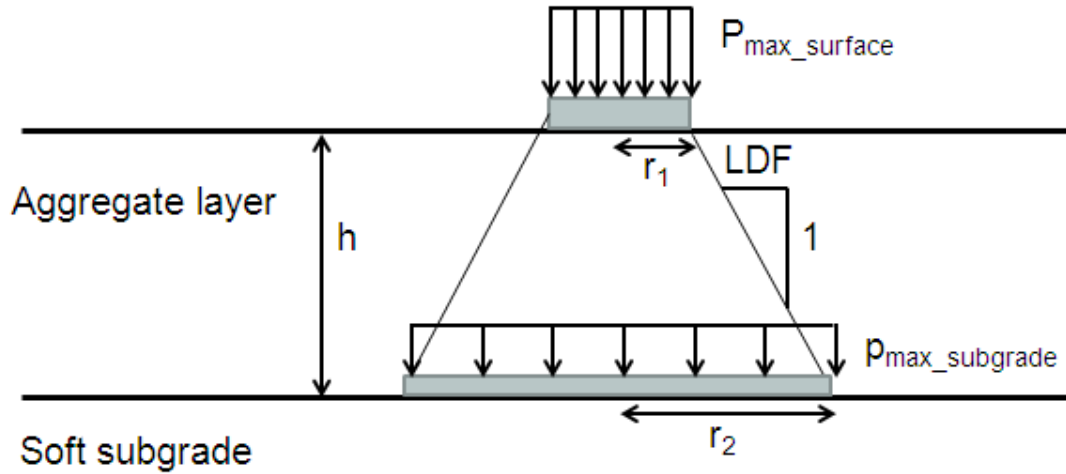


Figure 5.9 Definition of the load distribution factor LDF.

The fundamental idea of the proposed new design approach against Mode 2 rutting is that the ultimate wheel load W_{max} , determined by means of its respective Finite Element model calculation, is related to the undrained shear strength of the subgrade material according to Equation 5.1.

$$W_{max} = \pi \cdot r_1^2 \cdot p_{max\ surface} = \pi \cdot r_2^2 \cdot p_{max\ subgrade} = \pi \cdot (r_1 + h \cdot LDF)^2 \cdot 1.2 \cdot 5.14 \cdot s_u \quad (\text{Eq. 5.1})$$

where r_1 is radius of the loaded area on the road surface, $p_{max\ surface}$ is the maximum uniform vertical pressure on the road surface, r_2 is radius of the loaded area on the subgrade surface, $p_{max\ subgrade}$ is the maximum uniform vertical pressure on the subgrade surface, h is thickness of the aggregate layer, LDF is defined as in Figure 5.9, and s_u is undrained shear strength of the subgrade soil.

In the right side of Equation 5.1, the first part represents the assumed loaded area at the subgrade surface level, while the latter part is a direct application of a standard bearing capacity formula used in soil mechanics (e.g. Smolczyk 2003), assuming a shape factor value of 1.2 for a circular loading area, and a bearing capacity factor of 5.14 for the shear strength of a cohesive subgrade soil in undrained conditions. The balancing effect of the weight of aggregate material around the load distribution area, schematically indicated by the small grey arrows in Figure 5.1, is omitted here due to its relatively small overall importance.

The values of LDF can be directly back calculated from the FE modeling results using Equation 5.1 once the respective ultimate wheel loads have been determined. This can be done by defining a ‘failure’ condition on the load-deflection curves in figure 5.7. In this research the criteria has been somewhat arbitrarily defined as a 10.0 mm deflection of the road surface under the centre of the wheel loaded area. By comparing this definition to the examples given in Figure 5.7 it seems that at about this point the load-deflection curves tend to bend clearly downwards, but there is still some small margin to an immediate and total collapse of the structure. From a practical point of view surface rut development of 10 mm at one load application also feels to be a fairly reasonable definition for the failure condition of the structure.

5.5.2. Effect of aggregate and subgrade strength

If we simplify the shear strength of the aggregate material in one single number, we can analyze how the load distribution factor LDF depends on the quality of the aggregate material. In the following the aggregate strength is described, somewhat arbitrarily again, by the value of its effective shear strength when the normal stress is at the level of 250 kPa. It is of course obvious

that the actual stress level varies throughout the wheel loaded aggregate layer. In some points the stress level experienced is higher than 250 kPa, while in some other points it remains lower than that value. The selected value could, however, possibly be able to give a sort of representative value for each aggregate, especially in relation to the others. If the respective aggregate layer in practice can be assumed to be reasonably well drained, and the number of consecutive load applications is reasonable, the effective stress approach corresponding to the drained conditions should also be reasonably well justified.

The back calculated values of the load distribution factor LDF for 0.4 m thick structures are presented in Figure 5.10 as a function of aggregate shear strength determined as explained above. Based on this figure it seems fairly obvious that the load distribution taking place in the aggregate layer is better the higher the aggregate shear strength. On the practical range of variation of the aggregate shear strength the relation to LDF seems to be even fairly linear.

Another obvious remark from Figure 5.10 is that LDF is higher the weaker the subgrade material underlying the aggregate layer. In practical terms this could be explained that the weaker subgrade is forcing the load spreading aggregate material to its maximum performance to compensate for the inadequate properties of the subgrade. Quite clearly this is one more proof to the old well-known fact that a pavement structure should always be analyzed as one unity, and not as a structure consisting of separate components that do not have any interaction with each other.

The relation between LDF and undrained shear strength of the subgrade does not seem to be fully linear, but rather that the effect of subgrade strength is more pronounced when the subgrade material is extremely weak. A very logically trend, in fact. In figure 5.10 this is indicated by the shorter spacing between the two lowermost lines, compared to the respective distance between the two uppermost lines.

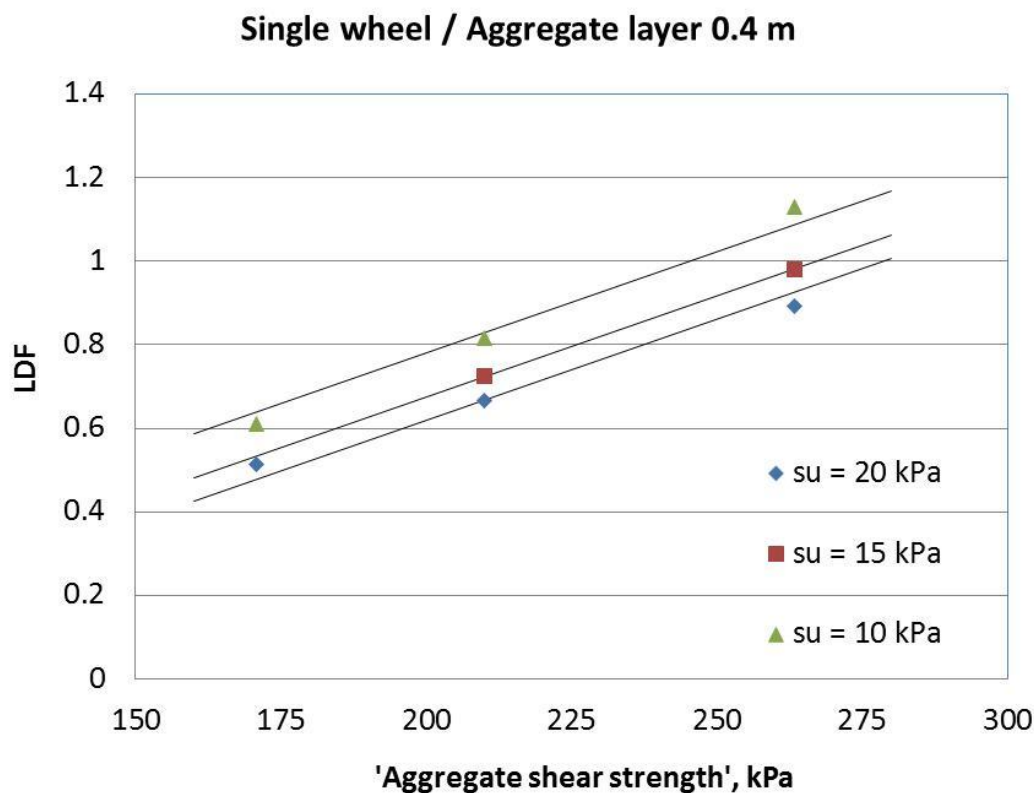


Figure 5.10 Load distribution factor LDF as a function of aggregate shear strength and undrained shear strength of the subgrade. In all of these analyses the aggregate layer thickness has been 0.4 m.

Even though the linear relation between aggregate shear strength and LDF seems to be fairly appropriate in Figure 5.10, a slightly better representation of the analysis results is achieved if the 'line fitting' is made using a set of lines starting from one single point close to the origin of the picture. In figure 5.11 this point has the coordinates (100, 0.2). In practice having a common origin for all lines logically means that the aggregate is losing its capacity for load spreading as its shear strength approaches zero.

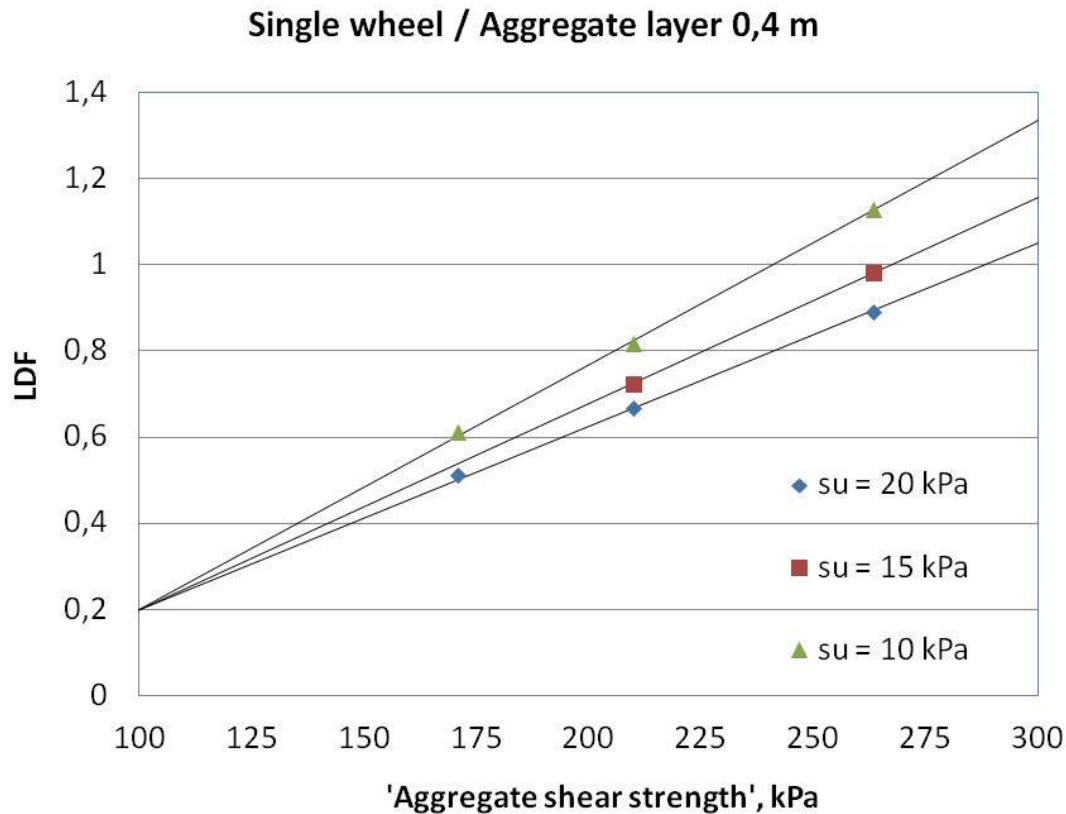


Figure 5.11 Load distribution factor LDF as a function of aggregate shear strength and undrained shear strength of the subgrade. The results have been described using a set of lines starting from the same point of origin.

5.5.3. Effect of aggregate layer thickness

In Figures 5.12 and 5.13 the load distribution factor LDF is again presented as a function of aggregate shear strength, but now a distinction is made between the different layer thicknesses while the undrained shear strength of the subgrade material remains constant.

The analyses clearly reveal that the relation between aggregate shear strength and LDF is again essentially linear, but that the values of LDF are getting higher the thinner the aggregate layer. A physical explanation for this could again be that when the aggregate layer is too thin on a weak subgrade, it is forced to its maximum performance when it tries to keep the whole structure 'in one piece'.

Also here it seems obvious that the effect of layer thickness is more pronounced when the aggregate layer is very thin, than when it has a reasonable thickness. The logic behind this trend could be analogous to that discussed above concerning the effect of subgrade shear strength.

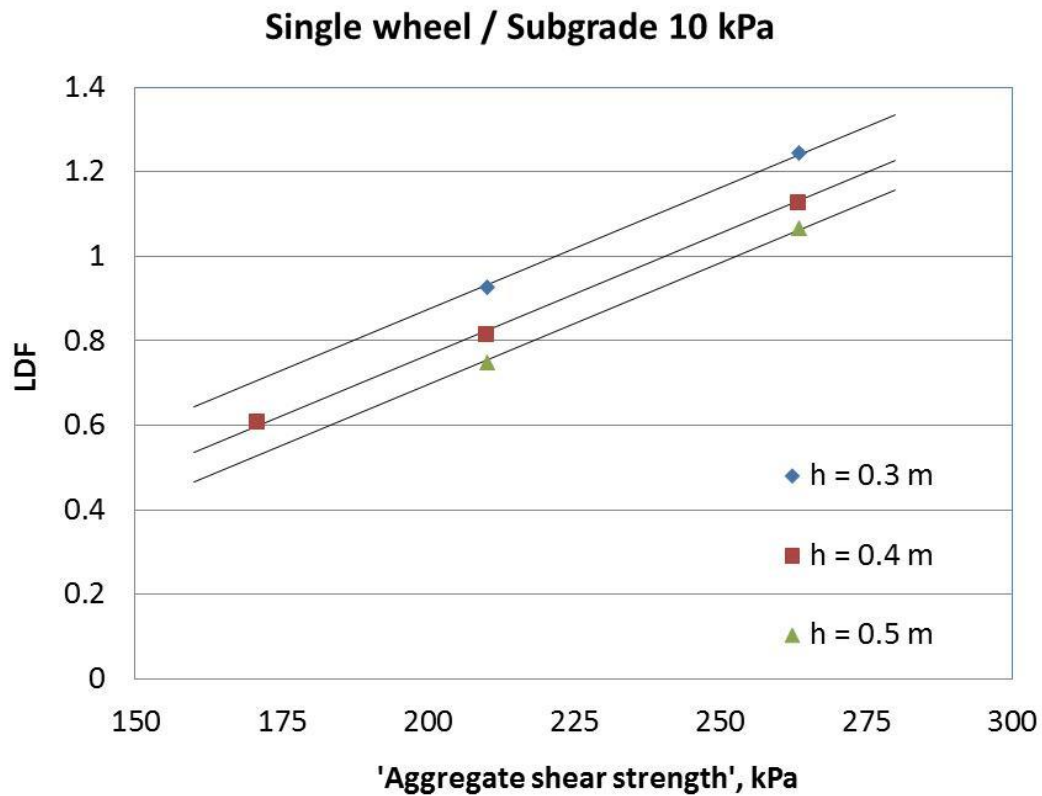


Figure 5.12 Load distribution factor *LDF* as a function of aggregate shear strength and aggregate layer thickness. In all of these analyses the undrained shear strength of the subgrade has been 10 kPa.

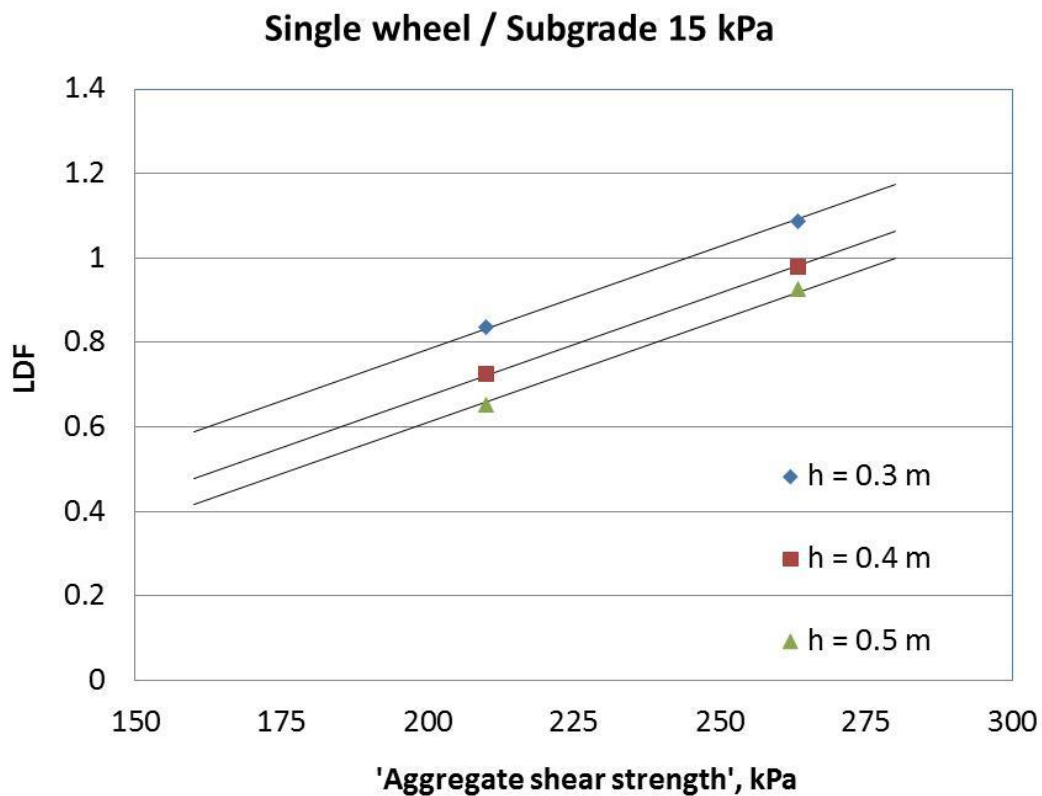


Figure 5.13 Load distribution factor *LDF* as a function of aggregate shear strength and aggregate layer thickness. In all of these analyses the undrained shear strength of the subgrade has been 15 kPa.

5.5.4. Effect of wheel configuration

While all of the above analyses have been made based on the assumption that the whole of the wheel load corresponding to half of the 100 kN standard axle load is transferred on the road surface via a single circular contact area representing a single wheel configuration. From practical point of view this is, however, a marked limitation, because in many cases dual wheel systems are used in heavy vehicles instead of a single wheel configuration. In this research the dual wheel loading situation was analyzed by constructing a similar FE model as the one shown in Figure 5.4, but with two circular loaded areas at a distance of 0.3 m apart from each other on top of it. At the same time the respective single wheel load was divided into two halves (2 x 25 kN) acting on each of the contact areas. Because the contact pressure was at the same level of 800 kPa, the radius of the contact area was reduced from 0.141 m to 0.100 m.

In terms of load distribution factor LDF, the result of the analysis is presented in Figure 5.14. When comparing the results with those shown for single wheel configuration in Figures 5.10 and 5.11 it is easy to recognize that the trends concerning both the effects of aggregate strength, and undrained shear strength of the subgrade material, are basically just the same. The absolute values of LDF are, however, somewhat lower for the dual wheel system in all of the analyzed combinations of aggregate and subgrade quality. An obvious practical explanation for this is that because the dual wheels are reasonably close to each other, the load distribution under both of the wheels cannot take place separately, but partly the load distributions combine. An example of the load distribution under a wheel load of 2 x 25 kN resting on a structure similar to that of Figures 5.4 and 5.5. is shown in Figure 5.15. The difference in the shapes of the load distribution between Figures 5.5 and 5.15 is obvious.

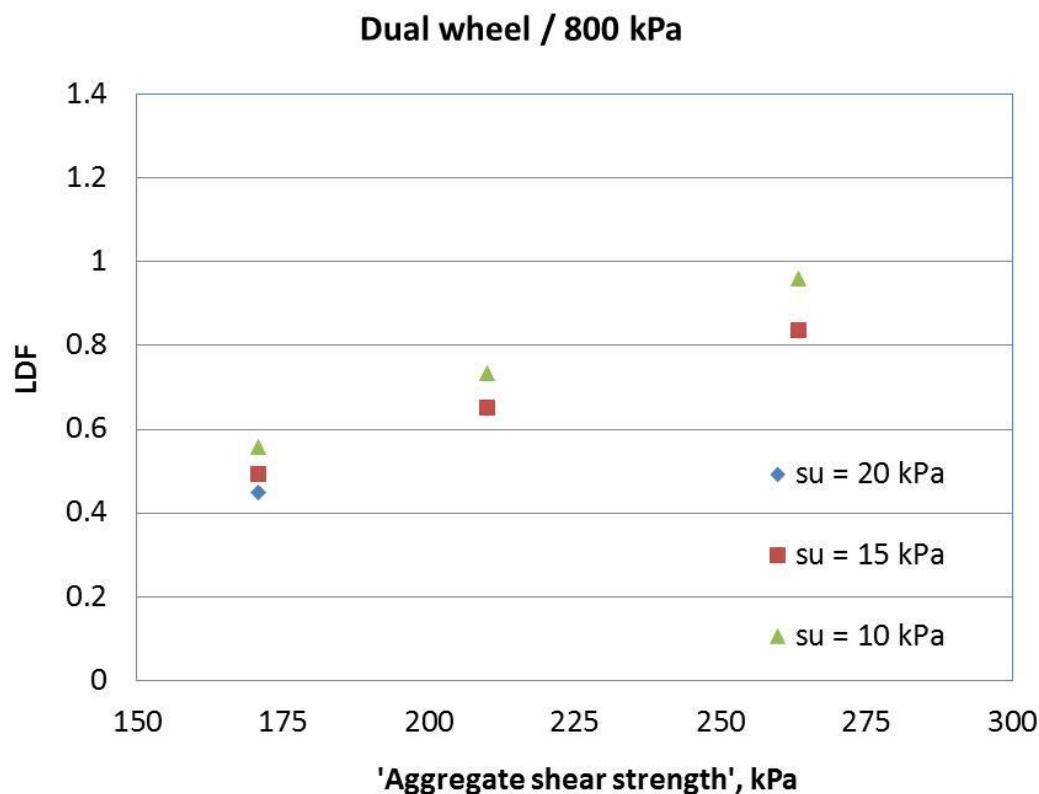


Figure 5.14 Load distribution factor LDF as a function of aggregate shear strength and undrained shear strength of the subgrade for a dual wheel system. In all of these analyses the aggregate layer thickness has been 0.4 m.

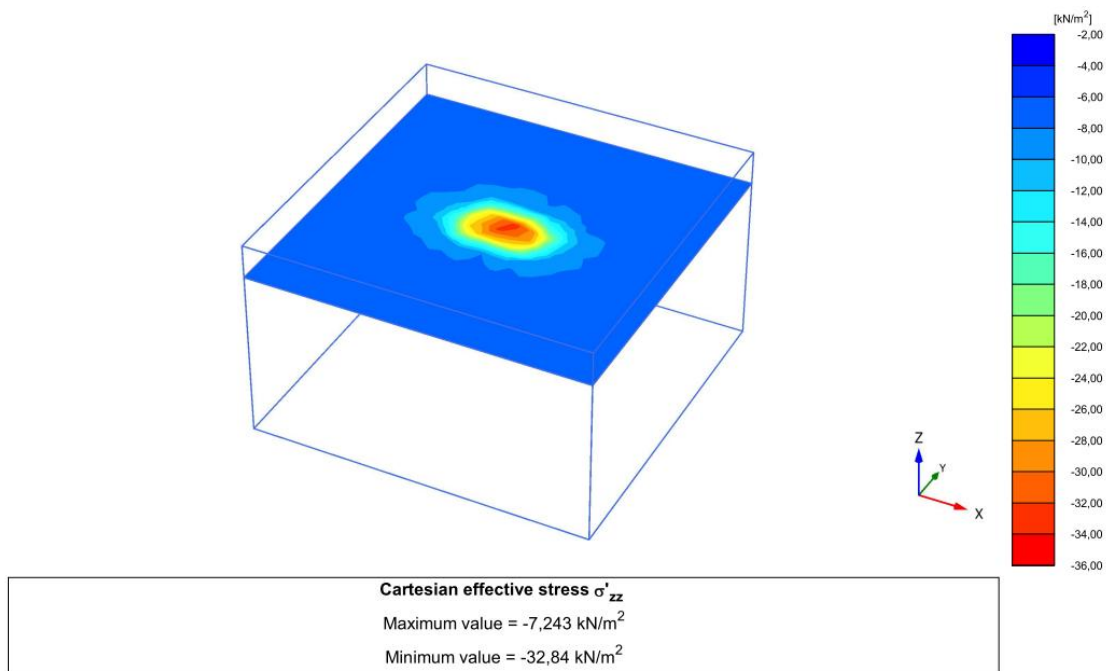


Figure 5.15 Distribution of vertical stresses in a plane located at the subgrade surface for a dual wheel configuration on a structure similar to that of Figure 5.4; undrained shear strength of the subgrade is 15 kPa.

Even though the number of analyses indicated by the coloured markers in Figure 5.14 is fairly limited, it seems that also in this case a sensible representation of the results can be achieved by using a set of lines starting from a common origin. In Figure 5.16 this origin has been chosen to be the same as in figure 5.11 for the single wheel configuration.

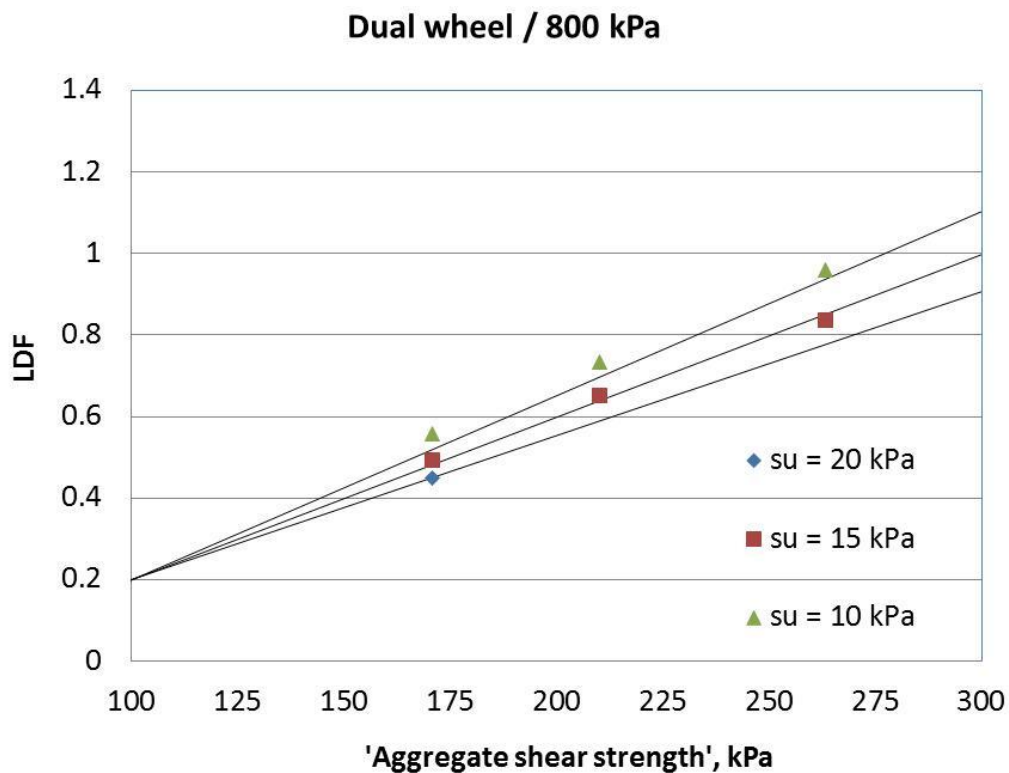


Figure 5.16 Load distribution factor LDF as a function of aggregate shear strength and undrained shear strength of the subgrade for a dual wheel system. The results have been described using a set of lines starting from the same origin.

5.5.5. Effect of tyre inflation pressure

The effect of tyre inflation pressure was investigated by analyzing the same combinations of aggregate quality and subgrade shear strength as above for dual wheel loading (Figures 5.14 and 5.16). In these analyses a dual wheel load configuration was also used, because from a practical point of view it was assumed that, on LVRs, a central tyre inflation (CTI) system was more likely to be installed in a vehicle equipped with dual wheels than super singles.

The results of the analyses are again summarized in terms of load distribution factor LDF in Figure 5.17. When comparing the results with those shown in Figure 5.16 for normal tyre inflation pressure of 800 kPa, we can see that there is some difference in the direction of LDF values for the tyre inflation pressure being lower, but the differences are still very small. In practical terms this means that as far as Mode 2 rutting is concerned the effect of lowering tyre inflation pressure by means of a CTI system on a structure with thickness of 400 mm or more is marginal – exactly as could be expected.

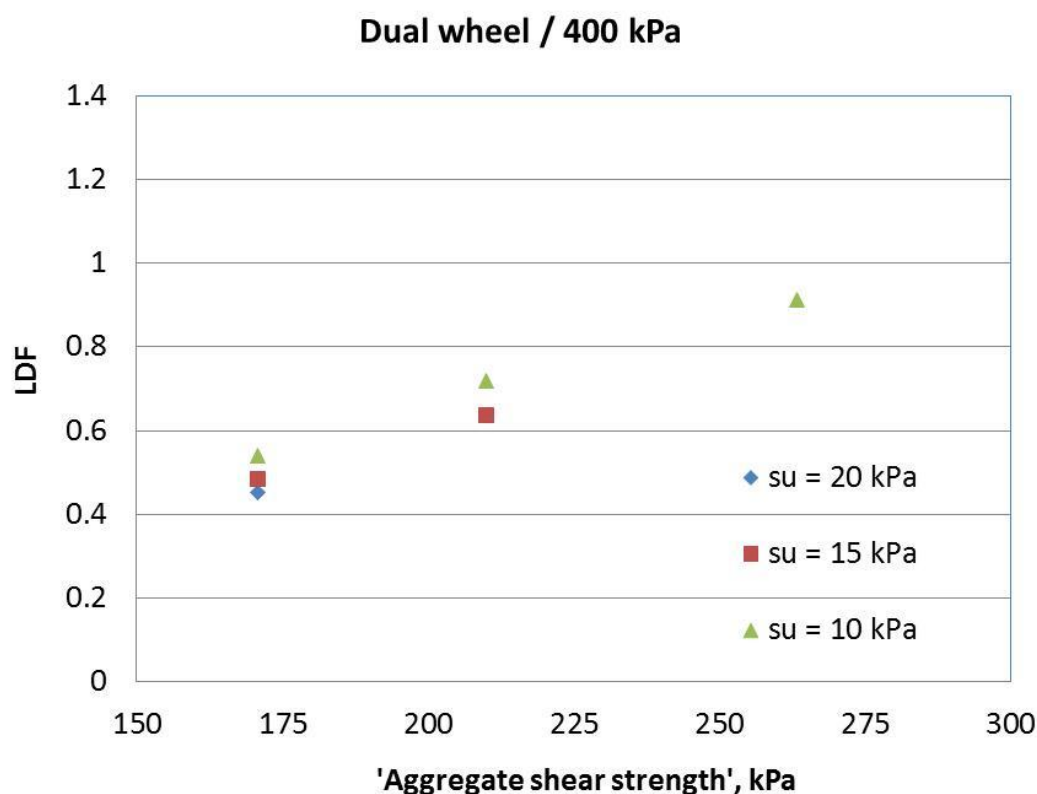


Figure 5.17 Load distribution factor *LDF* as a function of aggregate shear strength and undrained shear strength of the subgrade for a dual wheel system with a tyre inflation pressure of 400 kPa. In all of these analyses the aggregate layer thickness has been 0.4 m.

5.5.6. Final outcome of the new design approach development

As indicated in Equation 5.1 in Chapter 5.5.1 the ultimate wheel load value, W_{\max} , is related to the maximum load carrying capacity of the subgrade, via the thickness of the aggregate layer (h) decided as a result of the design, the undrained shear strength of the subgrade material determined by site investigations or estimated based on experience, and the Load Distribution Factor (LDF) which in turn depends primarily on the aggregate quality, but based on the above discussion also on the subgrade shear strength and thickness of the aggregate layer. The radius of the contact area between the wheel and the road surface (r_1) is not in practice included in the analysis, as based on Chapter 5.5.5, it was observed to have only a marginal effect on Mode 2 rutting of the subgrade. In this research the values for r_1 for single and dual wheels at 800 kPa tyre inflation pressure have been taken to be 0.141 m and 0.100 m respectively.

Description of the aggregate shear strength

In the suggested new design approach for Mode 2 rutting the description of the aggregate shear strength, $s_{\text{aggregate}}$, is based on its effective strength parameters cohesion, c' , and internal friction angle, φ' according to Equation 5.2.

$$s_{\text{aggregate}} = c' + 250 \tan \varphi' \quad (\text{Equation 5.2})$$

In practical terms this expression describes the effective shear strength of the material at a normal stress level of 250 kPa. Figure 5.18 provides values of the term $(250 \cdot \tan \varphi)$ directly in graphical form.

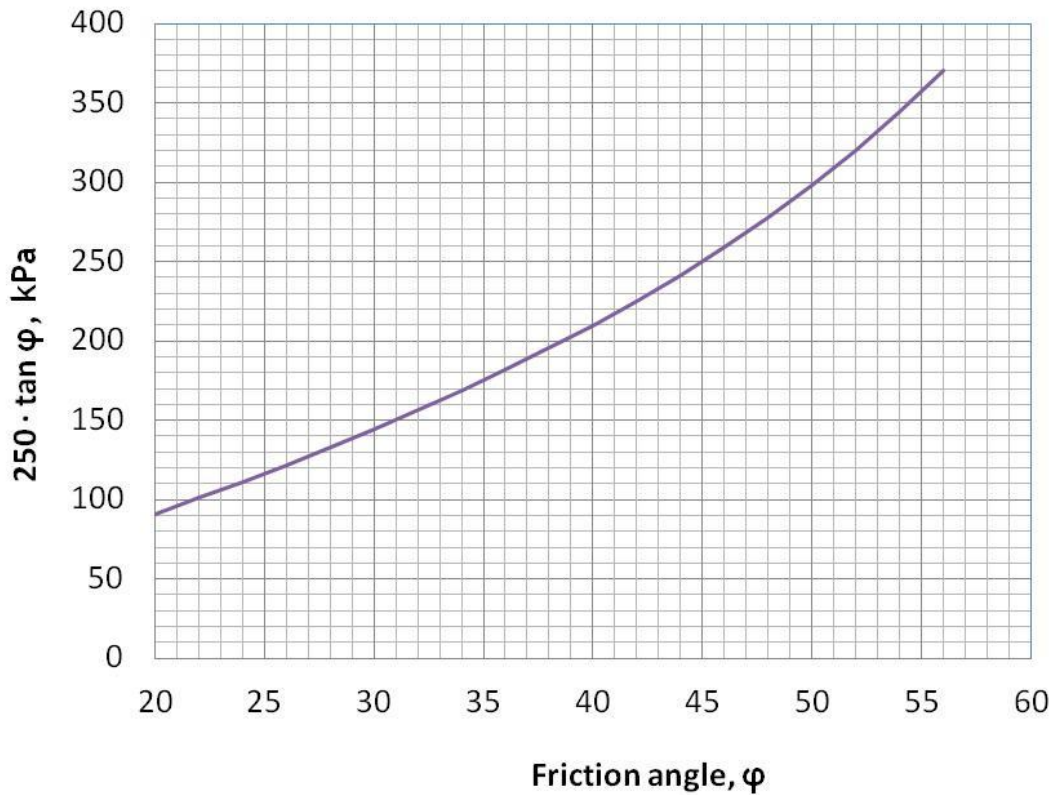


Figure 5.18 Values of the term $(250 \cdot \tan \varphi)$ as a function of friction angle φ .

Assessment of the value of LDF

It is suggested that the assessment of the Load Distribution Factor, LDF, for a single wheel loading should be based on figure 5.19 which is presented in the same fashion as Figure 5.11 as a function of aggregate shear strength, $s_{\text{aggregate}}$ and undrained shear strength of the subgrade soil $s_{u \text{ subgrade}}$. Similarly, for dual wheel loading it is suggested that the assessment should be based on Figure 5.20.

At this point it should be noted that in comparison to the analyses presented above, the results shown in Figures 5.19 and 5.20 have been slightly extrapolated beyond the range of 10 kPa to 20 kPa subgrade shear strength values in the Finite Element analyses. Any further extrapolation of the results should be exercised with marked caution.

The mathematical formulation of the set of lines presented in Figures 5.19 and 5.20 is given by Equation 5.3:

$$LDF_{\text{initial}} = A_i \cdot \frac{s_{\text{aggregate}}^{-100}}{1000} + 0.20 \quad (\text{Equation 5.3})$$

In this the value of parameter A_i has been determined based on curve fitting the Finite Element analysis results, and can be written as Equation 5.4 for single wheel configuration and Equation 5.5. for dual wheel configuration.

$$A_1 = 0.00785 \cdot (s_{u \text{ subgrade}})^2 - 0.37132 \cdot s_{u \text{ subgrade}} + 8.62417 \quad (\text{Equation 5.4})$$

$$A_2 = 0.00148 \cdot (s_{u \text{ subgrade}})^2 - 0.14166 \cdot s_{u \text{ subgrade}} + 5.78148 \quad (\text{Equation 5.5})$$

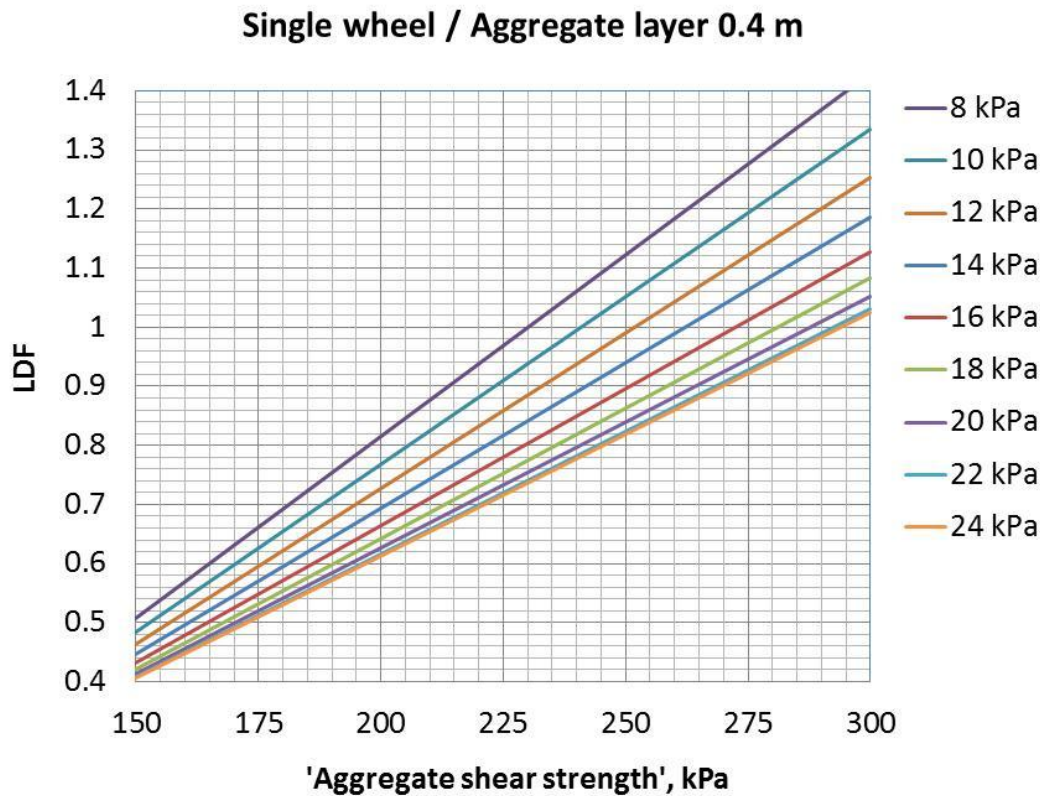


Figure 5.19 Assessment of the Load distribution factor LDF as a function of aggregate shear strength and undrained shear strength of the subgrade soil for single wheel configuration.

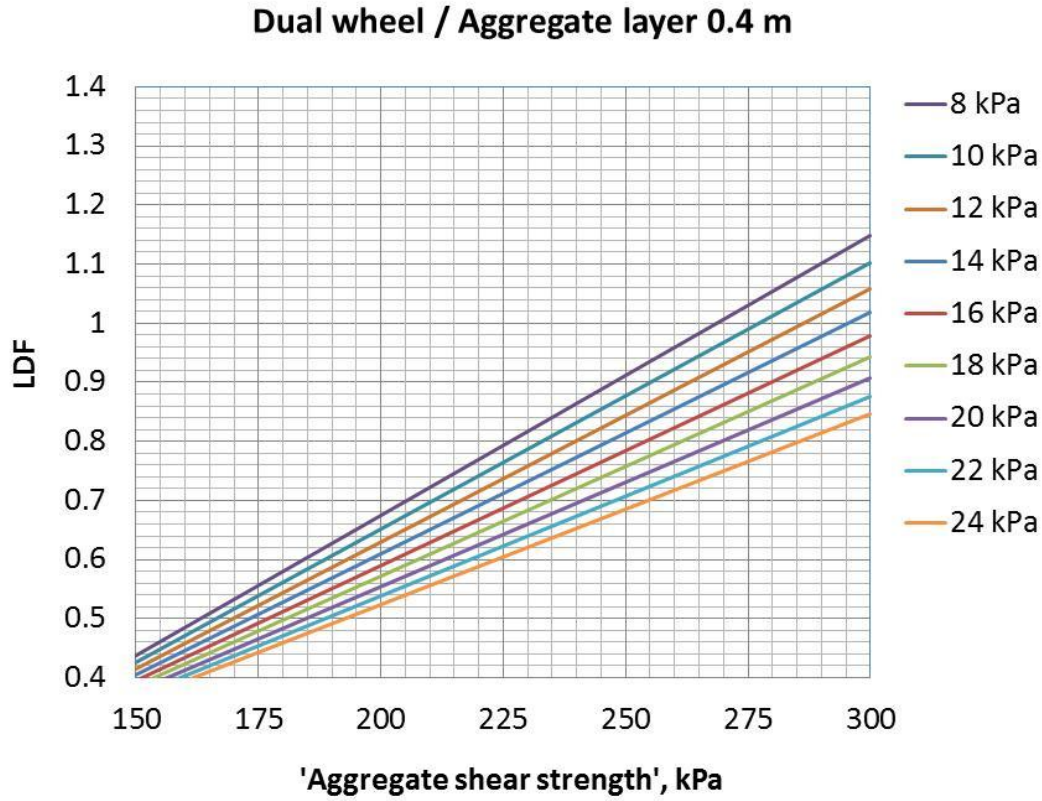


Figure 5.20 Assessment of the Load distribution factor LDF as a function of aggregate shear strength and undrained shear strength of the subgrade soil for dual wheel configuration.

Correction for the effect of aggregate layer thickness

As indicated in Chapter 5.5.3 above, the thickness of the aggregate layer on top of the subgrade has an obvious effect on the actual value of LDF. It is suggested that this effect should be taken into account by applying a correction increment ΔLDF to the value of $LDF_{initial}$ corresponding to the aggregate layer thickness of 0.4 m (Equation 5.3 and Figures 5.19 and 5.20). It is suggested that this correction should be made based on Figure 5.21, or Equation 5.6 below.

$$\Delta LDF = 2.0652 \cdot (h - 0.4)^2 - 0.8771 \cdot (h - 0.4) \quad (\text{Equation 5.6})$$

in which h is thickness of the aggregate layer.

Here it should be noted again that actual Finite Element analyses only covered the range of aggregate layer thicknesses from 0.3 m to 0.5 m, and thus any extrapolation of the results far beyond this range may be risky especially in the case of dual wheels.

The final value of LDF_{design} to be applied in the design is then given by Equation 5.7:

$$LDF_{design} = LDF_{initial} + \Delta LDF \quad (\text{Equation 5.7})$$

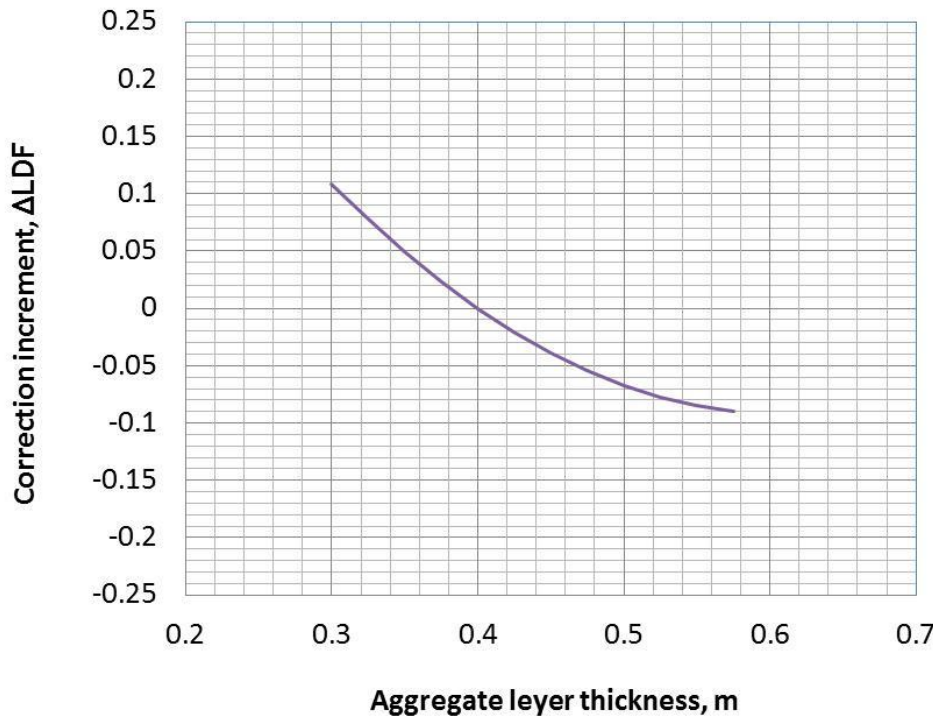


Figure 5.21 Assessment of correction increment ΔLDF into the initial value of Load distribution factor $LDF_{initial}$ to take into account the effect of aggregate layer thickness.

Inclusion of the safety margin

All of the above analyses are based on the criterion that was set for the failure condition of the combination of the aggregate layer and underlying subgrade in Chapter 5.5.1, i.e. a deflection of 10 mm of the road surface under one single load application - in this case calculated in accordance with Finite Element analyses. To prevent this situation arising, a safety margin should be provided against this condition. A practical way of introducing this safety margin into the analysis is to supplement Equation 5.1 with a factor of safety F_s . Thus we can rewrite it in the form of Equation 5.8 for single wheel configuration, and Equation 5.9 for dual wheel configuration, respectively:

$$W_{\max SW} = \frac{19.38}{F_s} \cdot (0.141 + h \cdot LDF_{SW})^2 \cdot s_u \quad (\text{Equation 5.8})$$

$$W_{\max DW} = 2 \cdot \frac{19.38}{F_s} \cdot (0.100 + h \cdot LDF_{DW})^2 \cdot s_u \quad (\text{Equation 5.9})$$

in which LDF_{SW} and LDF_{DW} have been determined according to the principles described above, $W_{\max SW}$ is the maximum value of the wheel load for single wheel configuration, and $W_{\max DW}$ is the maximum value for the combined wheel loading of the pair of dual wheels at one end of the axle.

The selection of the value of F_s is left to user of the design method, but as some sort of minimum a value of $F_s = 1.5$ is suggested. In normal cases, however, a higher margin of safety should be selected. An exception to this may be a condition in which the number of load applications is known to be very low, and the consequences of a possible structural failure of the road acceptable. In these conditions even a value of $F_s = 1.3$ may be considered.

Summary

The suggested new design approach against Mode 2 rutting of the subgrade should be performed as follows:

1. Define the design wheel/axle load, type of wheel configuration to be analysed and the total factor of safety to be applied in the analysis
2. Assess the undrained shear strength of the subgrade material, $s_{u \text{ subgrade}}$ (see Chapter 6)
3. Assess the effective shear strength parameters of the aggregate material to be used, taking into account the expected conditions of the site (see Chapter 6), and transform these values as a value of $s_{\text{aggregate}}$
4. Select a preliminary value for aggregate layer thickness, h
5. Based on $s_{u \text{ subgrade}}$ and $s_{\text{aggregate}}$ determine the value of LDF_{initial}
6. Based on the selected value of h determine the values of ΔLDF and LDF_{design}
7. Apply Equation 5.8 or 5.9 to determine the maximum allowable wheel load
8. If the requirements for the design are met, return to point 4 to optimize the aggregate layer thickness h . If not, return to point 4 and try with a higher value of h .

If the design criteria are not met with a reasonable layer thickness h , the following possibilities could be considered:

- Using a lower value of design wheel/axle load (i.e. application of a weight restriction).
- Improving the quality of the aggregate material to be used, either by processing the original one or changing it to a different one.
- Improving the properties of the subgrade material by ground improvement techniques, or by replacing the subgrade material.
- Using reinforcement in the base / lower part of the aggregate layer. Analysis of this type of structural solutions is, however, not covered by the design approach presented in this report.

Some examples of applying the suggested design approach in practical design considerations are given in Appendix 1 of this report.

6. DETERMINATION OF THE DESIGN PARAMETERS

Both of the suggested new design approaches against Mode 1 and Mode 2 type of rutting require strength properties of the aggregate material as input values. Unlike stiffness properties of aggregate materials, the evaluation of strength parameters for different types of coarse grained aggregate materials is unlikely to be a task with which most engineers dealing with the design of low volume roads are familiar with. A further difficulty in assessing strength parameters to be used in Mode 2 rutting analysis is that the values of shear strength parameters cohesion “ c ” and friction angle “ ϕ ” typically used in the geotechnical design of foundation engineering structures are not necessarily applicable for the structural design of LVRs due to the differences in the levels of stresses and strains involved, and at least to some extent also to the different requirements for safety margins against total failure conditions.

Normally the mechanical properties of aggregate and subgrade materials are determined by laboratory and site investigations methods, both direct and indirect methods. A discussion of these follows.

6.1. DIRECT LABORATORY METHODS

6.1.1. Triaxial testing

The most widely used direct experimental test for the mechanical properties of aggregates and soil materials is the triaxial test. Depending on the material being tested, especially the maximum grain size of the material, different scales of equipment are used. In the case of coarse grained aggregate, material test specimen diameters of up to 200 mm and 300 mm are needed. This requirement, however, makes the testing fairly expensive and the testing equipment hard to find.

A reasonably extensive series of large scale triaxial tests was performed at the Tampere University of Technology in connection with the ROADDEX project using different types of aggregate materials from Finland, Sweden and Scotland. The aim of the test series was to provide a basic data set of design parameters that could be used in assessing design parameters case by case based on a simple index type of tests, where it was not possible to carry out case specific testing by more sophisticated means. The outcome of this research effort is explained in more detail in chapter 6.4.

The basic idea in triaxial testing is to expose a cylindrical test specimen that is surrounded by a rubber membrane under an axisymmetric stress state in a pressure chamber filled with air or liquid. In normal test setups the specimen is then loaded by changing the axial stresses acting on the specimen by a “monotonously increasing”, or a cyclic (i.e. repeated), loading depending on the aim of the test. The drainage conditions of the specimen can also be controlled during the test so as to make it possible to simulate both drained and undrained in-situ conditions. Figure 6.1 shows the large scale triaxial testing facility available at the Tampere University of Technology that was used in this research. More details on triaxial testing reference can be found in the abundant literature available elsewhere.



Figure 6.1 Large scale repeated loading triaxial testing facility in the Laboratory of Earth and Foundation Structures of the Tampere University of Technology.

The normal procedure in determining the shear strength of a coarse drained material is to make a series of identical test specimens and then expose them to a monotonous increasing axial load until failure under different confining pressures within the test chamber. This of course makes the testing even more laborious and expensive as a fresh test specimen is required for every confining pressure level. In this research, however, a so called multi-stage testing approach was utilized. This meant that the testing was started at the lowest value of confining pressure as normally, but the monotonously increasing axial loading was suspended as the specimen started to yield under a constant axial load. After removing the axial load (deviator stress), the confining pressure was then increased to the next level and the procedure repeated again. By this means the shear strength determination could be made with up to four different values of confining pressure by using just one single test specimen (Figure 6.2).

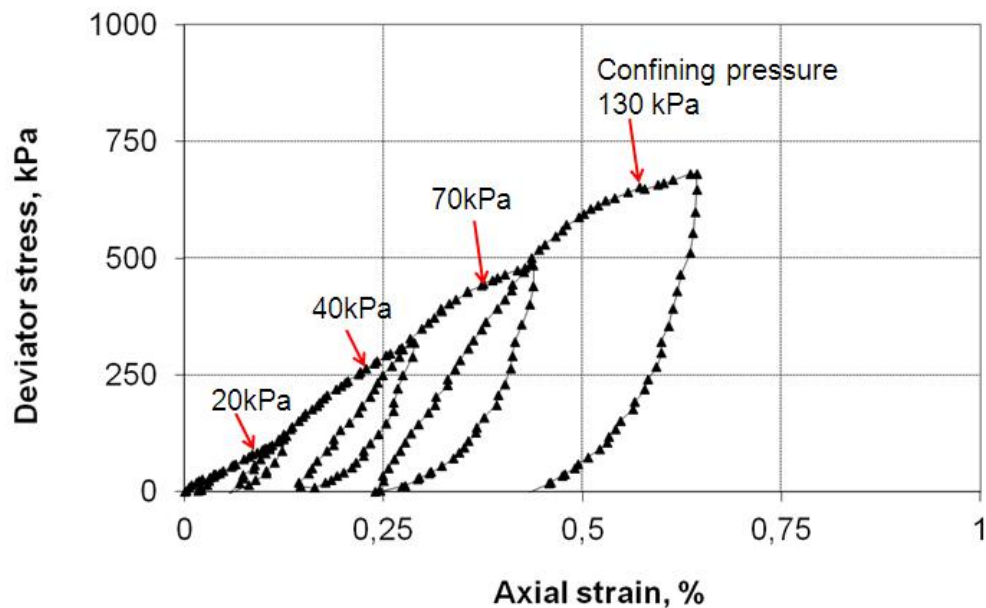


Figure 6.2 An example of the test procedure in a multi-stage monotonic loading triaxial test.

A cyclic (i.e. repeated) load is normally used when the aim of the test is to determine the resilient deformation properties (i.e. stiffness) of an aggregate material. In many respects the main principles of the loading arrangement are exactly the same, the main differences being in the loading frequency on which the specimen is exposed to (normally up to 10 Hz) and the requirements concerning the accuracy of strain measurements made from the specimen. More details on these issues can be found in the related literature (e.g. in Kolisoja 1997).

6.1.2. Other laboratory methods

Other laboratory methods are available for the direct determination of undrained shear strength properties of the more fine grained materials. These include fall cone test, undrained triaxial test and direct shear test, the latter one of which is to some extent used also for testing of more coarse grained materials. An important prerequisite for using any of these methods is, however, the availability of undisturbed soil samples taken in-situ. A more detailed description of these methods can again be found in the abundantly available literature on general soil mechanics and the respective testing standards.

6.2. INDIRECT LABORATORY METHODS

The limitations of available time and money for LVRs however mean that the evaluation of the mechanical properties of aggregate materials must in many cases be made based on indirect methods. That is to say that the property, e.g. shear strength of a material, is not measured directly by using appropriate test methods, but is correlated to some other technical properties of the material based on earlier experience. Quite often these correlations make use of the grain size distribution of the materials, because it is normally fairly easy and straightforward to determine, provided that representative samples of the material are available.

Another quite frequently applied method for assessment of the aggregate material quality is the Tube Suction (TS) test. In the TS test water is allowed to soak into a test specimen that has been previously dried in an equilibrium moisture content corresponding to very dry seasonal conditions. The speed and amount of water absorption into the test specimen is monitored by using the measurement of dielectric value of the specimen surface as shown in Figure 6.3.



Figure 6.3 Measurement of the dielectric value of a Tube Suction test specimen.

6.3. SITE INVESTIGATIONS

6.3.1. Shear vane test

The most widely used equipment for direct measurement of the undrained shear strength of soft subgrade soils is the shear vane. The method is internationally standardized and most site investigation contractors have the equipment readily available, at least in the Scandinavian countries. The main drawback concerning the extensive use of the shear vane method is obviously the cost. Shear vane tests are fairly time consuming to perform and thus also relatively expensive.

6.3.2. Dynamic Cone Penetrometer, DCP

The Dynamic Cone Penetrometer, DCP, is a simple, hand operated site investigation tool increasingly used in the Northern Periphery areas to assess the mechanical properties of road structures and underlying subgrade (Figure 6.4). Most often the interpretation of the penetration resistance is made in terms of the stiffness properties of the penetrated material (Figure 6.5) but it should also be possible to develop the same type of correlations between the penetration resistance and strength properties of the material. In fact, the DCP method as such is more directly a strength measurement rather than stiffness measurement, because as the penetrometer tip is forced into the aggregate or soil material a failure condition needs to be developed in the material surrounding the tip.

An even more important drawback concerning the assessment of undrained shear strength of soft subgrade soils by DCP is that most of the existing experience on the use of the device is from aggregates or other types of stiffer materials. To some extent DCP device may not even be sensitive enough to distinguish small differences in the strength properties of soft soils due to its too high penetration capacity.

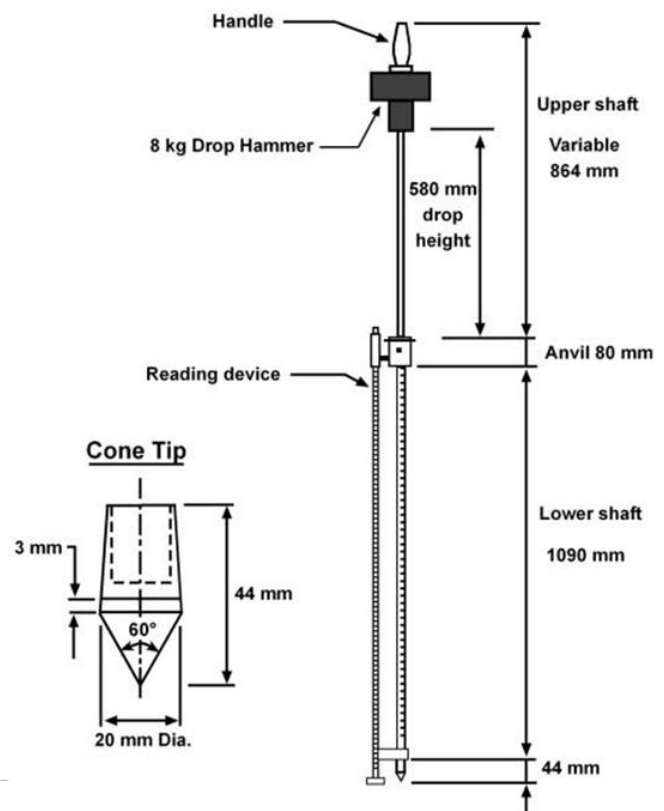


Figure 6.4 Dynamic Cone Penetrometer in operation (left) and the equipment schematics (right).

An attempt was made to collect more experience on the use of DCP test method in the ROAD EX IV project in the assessment of the mechanical properties of a thawing subgrade soil under a low volume road. The research compared the results obtained with DCP to those obtained simultaneously by means of Falling Weight Deflectometer measurements. This part of the research was carried out and reported by the geotechnical research group of the Technical University of Luleå in Sweden under the supervision of professor Sven Knutson.

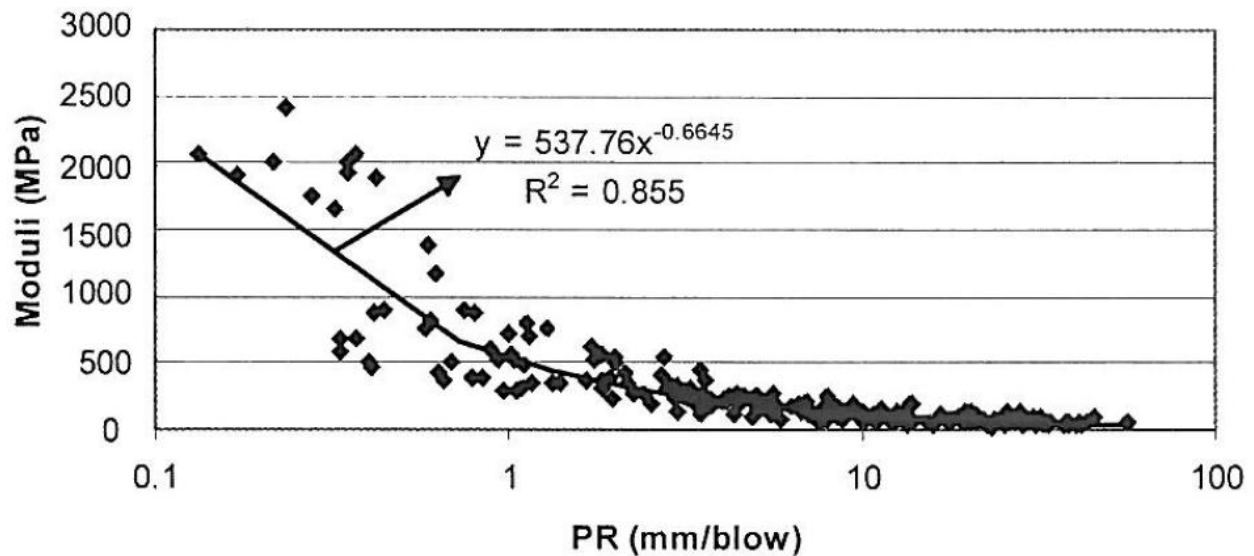


Figure 6.5 Correlation between the DCP penetration rate (mm/blow) and pavement material stiffness according to Chen et al. (2005).

6.3.3. Other sounding methods

In addition to the shear vane test there is a number of other site investigation tools routinely used in geotechnical explorations that can give very valuable information on the mechanical properties of subgrade soils, that can be used in Mode 2 rutting design. Two of the most well known and extensively used methods are the Cone Penetration Test (CPT) and Swedish Weight Sounding. While the first mentioned provides a more direct measurement of the actual shear strength of a cohesive subgrade soil, the main advantage of the latter is the extensive empirical knowledge available for the interpretation of its results.

Both of the above mentioned methods are described in detail in the Technical Specifications of the European structural design codes (CEN ISO/TS 22476:10).

6.3.4. Falling Weight Deflectometer

The Falling Weight Deflectometer, FWD, is an extensively used investigation tool for assessing the structural performance of existing road infrastructure. The main shortcoming in the applicability of this method in the search for design parameters for Mode 1 and Mode 2 rutting design is that it primarily measures **stiffness** of the structural layers and the underlying subgrade, but not their strength properties which need to be assessed at best based on empirical correlations only. The same shortcoming applies even more to the various types of light versions of the FWD device available on the market.

6.4. SUGGESTED VALUES OF SHEAR STRENGTH PARAMETERS BASED ON ROAD EX RESULTS

The test series referred to in Chapter 6.1.1 above altogether comprised 26 test specimens that were exposed to multi-stage monotonous loading triaxial testing in the large scale testing facility at the Tampere University of Technology. The test materials included reasonable quality crushed rock aggregates from Finland, a good quality crushed rock aggregate from Sweden and a mica-rich poor quality crushed rock aggregate from Scotland. In addition, one of the test materials was taken from an existing Finnish low volume road. This was used in a mixture with virgin crushed rock aggregate so as to simulate a typical condition in the field where an existing road is rehabilitated by adding new aggregate that is mixed over time with the old one. The most important technical parameters of the test materials are summarized in Table 6.1 and the grain size distributions of the original test material are shown in Figure 6.6. Table 6.2 provides a summary of the values of the most important technical properties of the triaxial test specimens. The main variables in the test series, in addition to the material type and origin, were fines content, compaction level and moisture content, as shown in Table 6.2.

Table 6.1 Main technical parameters of the aggregates used in the triaxial test series.

Material origin	Sweden	Finland I	Finland II	Scotland
Material type	0/32 mm CR	0/32 mm CR*	0/32 mm CR**	0/32 mm CR
Dry density (TS test), kg/m ³	2070	2280*	2140-2200	2270
Dielectric value E_{r_max}	6.9	13*	22 – 39	22
Conductivity, microS/c	20	74*	200 - 500	700
w (at the end of TS test), %	3.9	3.4*	5.5 – 7.1	6.3
Specific surface area, m ² /kg	2274	4158*	3900 – 6500	4636
Adsorption index	1.47	1.79*	2.25 – 2.62	2.79
LA value	30	-	-	30
Nordic ball mill value	23.2	-	-	44

*) tests made with 0/16 mm material taken from a storage heap

**) material from the base course of an existing road

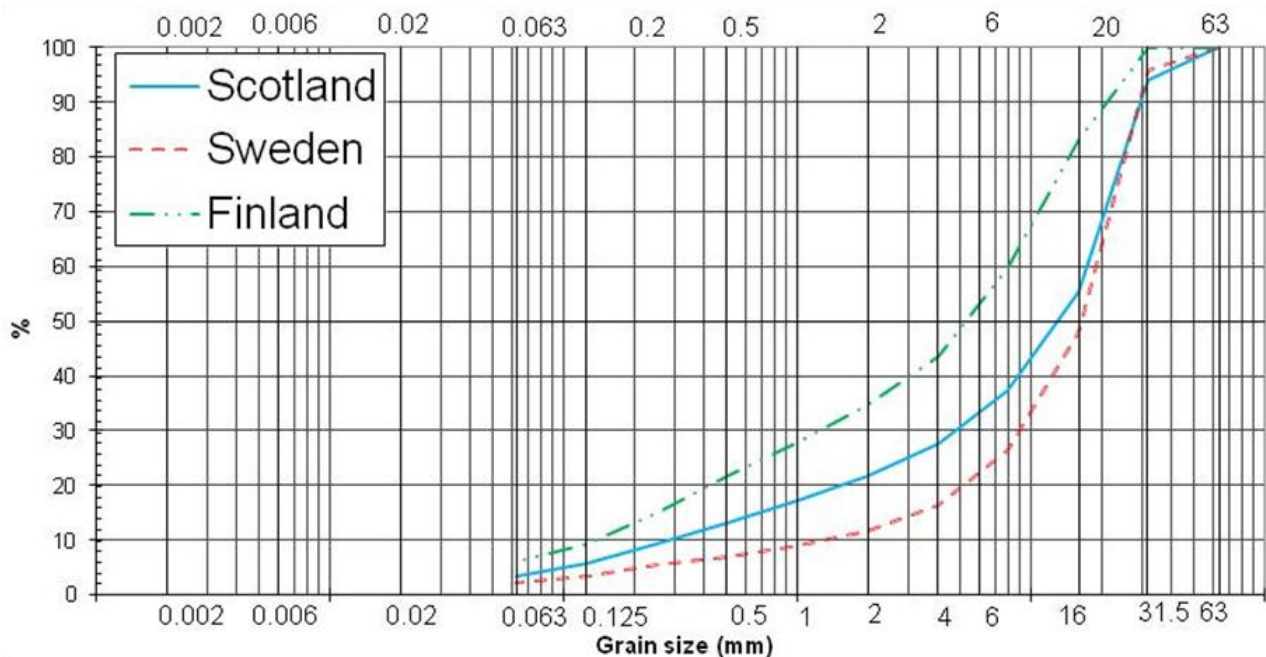


Figure 6.6 Grain size distributions of the original aggregate materials used in the triaxial test series.

Table 6.2 Technical properties of the triaxial test specimen.

Test specimen ID code	Test material	Amount of fines (<0.063 mm), %	Water content, %	Dry density, kg/m ³
E01_1	Sweden	2.8	3.0	2000
E01_2	Sweden	2.3	13.4	1950
E01_3	Sweden	3.1	3.0	1880
E01_4	Sweden	2.9	14.2	1880
E09_1	Scotland	5.0	4.7 ?	2130
E09_2	Scotland	5.9	8.1	2150
E09_3	Scotland	4.7	4.0	1970
E09_4	Scotland	4.7	12.5	1970
E09_5	Scotland	9.1	4.6	2100
E09_6	Scotland	6.9	9.4	2100
E09_7	Scotland	no	9.0	2140
E17_1	Finland I	6.5	5.2	2150
E17_2	Finland I	6.7	7.7	2090
E17_3	Finland I	6.1	4.2	1990
E17_4	Finland I	6.3	10.0	2000
E17_5	Finland I	9.2	4.0	2140
E17_6	Finland I	9.4	8.0	2160
E17_7	Finland I *	8.1	"6.8"	2200
E17_8	Finland I *	8.1	9.9	2060
E17_9	Finland I *	10.2	6.6	2210
E17_10	Finland I *	10.5	8.8	2120
E17_11	Finland I	8.0	11.0	2040
E17_A1-3	Finland I **	-	9.5	2070
E17_A4-6	Finland I **	-	5.0	2070
F09_1	Finland II	6.8	7.3	2190
F09_2	Finland II	7.5	10.8	2070

*) material from the wearing course of an existing road added

**) tests made with 0/20 mm fraction of the original aggregate (Finland I)

Based on the triaxial test results, shear strength parameters were derived for the good quality Swedish aggregate with a low fines content as shown in Figure 6.7. The figure shows the actual test results with red circles for the test material in two different compaction levels (thick / thin lines), and two different moisture contents (solid / dotted lines). The figure also indicates with a thick purple line an interpretation of the test results in terms of effective strength parameters $c' = 10$ kPa and $\phi' = 37.5^\circ$ for test specimen "E01_4" that had a high water content and low compaction level.

The artificial variation of the fines content of the test materials resulted in some cases where more than one test material behaved more or less similarly. The Tube Suction (TS) tests results obtained with each of the original aggregates, and the actual fines contents of the test specimens, were then used to classify the materials into three quality groups according to their mechanical performance – "good", "medium" and "poor" aggregates (see Table 6.3).

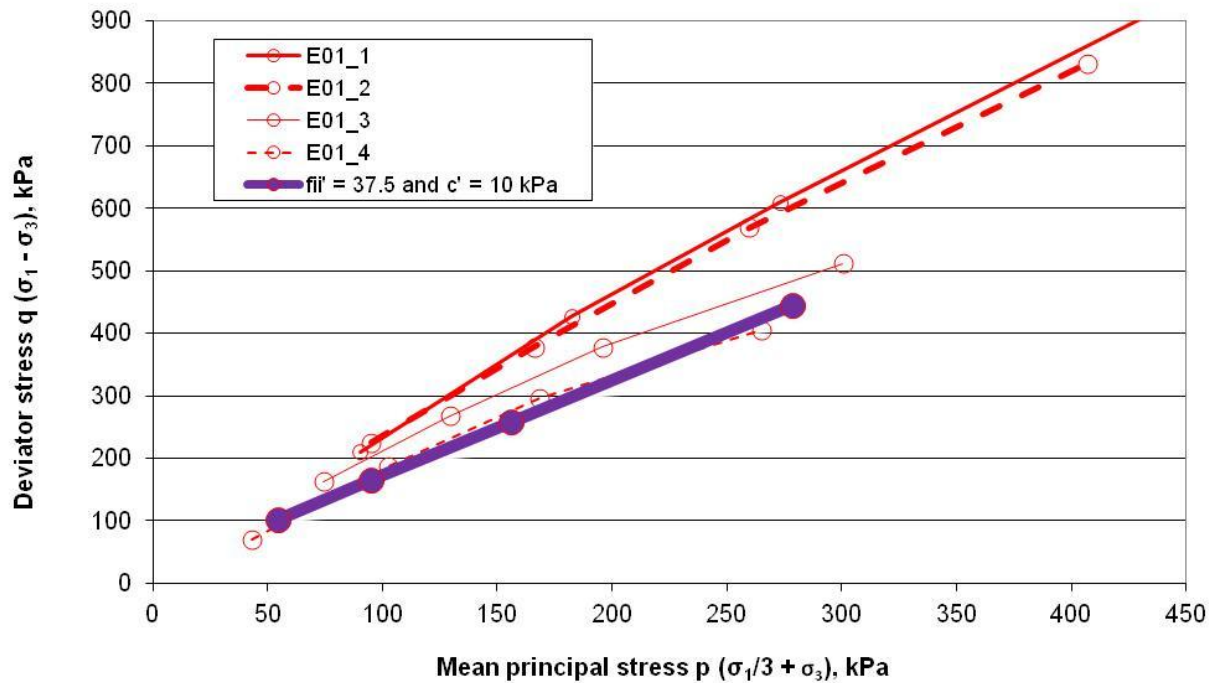


Figure 6.7 Monotonous loading triaxial test results for the good quality Swedish crushed rock aggregate and interpretation of the effective strength parameters cohesion, c' , and friction angle, ϕ' , for the material in low compaction level and high water content.

The shear strength parameter values obtained as above are summarized in Table 6.3. When using these parameters it is important to note that in some cases they represent a rough average, even within a group of test results, and not necessarily direct measurements from any of the actual test specimens. Despite this, it is hoped that the values will assist the user to make a rough estimate of the possible magnitudes of the parameter values if no other more detailed information is available. It must however be clearly stated that the final responsibility for the selection of any parameters in a design is on the designer alone, and that the author of this report cannot take any responsibility for the use of the parameter values shown in Table 6.3, or the conclusions based on them.

Table 6.3 Summary of the results of the multi-stage monotonous loading triaxial tests.

Material quality	Moisture content	Compaction level	Cohesion, c'	Friction angle, ϕ'
Good	Normal	OK / Appropriate	25	50
Good	Normal	Not Ok / Inappropriate	25	37.5
Good	High	OK / Appropriate	10	50
Good	High	Not Ok / Inappropriate	10	37.5
Medium	Normal	OK / Appropriate	10	45
Medium	Normal	Not Ok / Inappropriate	10	30
Medium	High	OK / Appropriate	5	45
Medium	High	Not Ok / Inappropriate	5	30
Poor	Normal	OK / Appropriate	10	40
Poor	Normal	Not Ok / Inappropriate	10	22.5
Poor	High	OK / Appropriate	0	40
Poor	High	Not Ok / Inappropriate	0	22.5

Definition of good quality aggregate

In the above classification the criteria for good quality aggregate can be defined as follows:

- Tube Suction (TS) test result $E_r < 9$, **and**
- Fines content $< 5\%$,**and**
- Material does not contain mica or other weathering minerals.

Additional criteria that can also be considered include:

- Specific surface area of fines $< 3000 \text{ m}^2/\text{kg}$
- Water adsorption index < 2

Definition of medium quality aggregate

Similarly, the criteria for medium quality aggregate can be defined as follows:

- TS-test result $9 < E_r < 16$, **and**
- Fines content $< 12\%$
- If material contains high amount of mica or other poor quality weathering minerals, fines content $< 7\%$

Definition of poor quality aggregate

If the material fails to fulfill the criteria for good or medium quality, it should be considered to be of poor quality, i.e.:

- TS-test result $E_r > 16$, **or**
- Fines content $> 12\%$.
- If the material contains a high amount of mica or other poor quality weathering minerals, fines content $> 7\%$

Effect of moisture content

Table 6.3 describes moisture content by the expressions of 'normal' and 'high' unlike Table 6.2 which lists the respective numerical values of the amounts of water contained in the test specimens in relation to the mass of dry aggregate material. In practical terms the definition 'normal' means that the amount of water contained in the aggregate is clearly lower than the maximum amount that the aggregate can retain in itself under the action of gravity. The definition 'high' in turn means that the aggregate has first been saturated and then allowed to drain during the triaxial test loading phase through the top of the test specimen.

When considering the effect of moisture content on the shear strength parameters of the tested aggregates it is important to note that in both of the testing conditions described above, the test had been started almost immediately after the test specimen had been compacted, and in the case of 'high' moisture content allowed to drain. This meant that the samples had not been exposed to any drying-wetting cycles which in practice, as a result of the suction effect, would have had a marked effect on the effective stress state of the material especially when it was drying. In terms of effective stress parameters this effect can primarily be interpreted as an increase in the value of apparent cohesion in comparison to the values indicated in Table 6.3. The practical importance of this issue, i.e. the importance of proper drainage of low volume road structures, is exemplified in the design examples given in Appendix 1.

Effect of compaction level

In Table 6.3 above, the test specimens have also been given the qualitative density descriptions of 'Ok/Appropriate' and 'Not Ok/Inappropriate'. The difference is in the amount of compaction effort given to the triaxial test specimen during the specimen preparation. In the case of 'Ok/Appropriate' the compaction effort was such that, based on earlier experience, the materials were close to the maximum compaction level that could be achieved using a vibratory compaction device weighing 1 kN, whilst in the 'Not Ok/Inappropriate' case the compaction time per layer was only about 20 % of the time of the 'Ok/Appropriate'. The respective values of dry density actually achieved with each of the test specimens are listed in Table 6.2.

7. CONCLUSIONS AND RECOMMENDATIONS FOR FUTURE WORK

This report gives a brief summary of the work done in the ROADDEX II project on the classification of rutting phenomena that typically take place on the LVR networks of the Northern Periphery. It then summarises the design approach developed primarily by the University of Nottingham during the ROADDEX III project against Mode 1 rutting, i.e. the rutting of the structural layers. The report then builds on these works and presents a new design approach against Mode 2 rutting, i.e. the rutting of the subgrade soil under a LVR having fairly thin structural layers composed of coarse grained aggregate material.

Development of the new design approach is based on the basic ideas put forward earlier during the earlier phases of ROADDEX and extended using advances in technologies now available to ROADDEX IV. These enhanced numerical modeling tools have enabled a much more sophisticated and, at the same time, realistic modeling of the mechanical behaviour of the structural system consisting of the aggregate material and the underlying subgrade soil. The design approach now developed is primarily based on analyzing the load distribution along the aggregate layer so as to assess how wide the area of tyre contact pressure, acting on the road surface, is distributed at the subgrade surface level. After that, a standard geotechnical bearing capacity formula is applied to assess the ultimate load carrying capacity of the subgrade soil, i.e. its ability to resist very rapid accumulation of permanent deformations under a small number of heavy wheel loads moving along the road surface.

It is important to note that, at this point, the new design approach is based on back calculating the results of Finite Element modeling in such a way that the same result in terms of ultimate load carrying capacity of the subgrade soil is achieved by a simple hand calculation procedure as would be obtained by making a sophisticated 3D Finite Element modeling of the combination of loading arrangement and road structure system at hand. Even though the new approach seems to be able to take into account the effects of key variables in a very logical manner it is important to acknowledge that the design approach is essentially based on adjusting the calculation procedure with a set of FE modeling results. Therefore, in future work it would be very important to verify the design approach by full-scale tests to be performed in-situ and based on them to make the required refinements into the calculation procedure.

Further work is also called for in making more sensitivity analyses on the effects of variables considered to have a minor importance in connection with this research. These include at least the effects of aggregate stiffness, subgrade soil stiffness and the relation between these two quantities. In addition, the effects of especially wide “maxi tyres” and the actual shape of contact the area between the tyre and road surface should also be studied in more detail.

An important step in the future work would also be to implement the design approach in the form of an easy-to-use software tool. Even though the required calculations in the present version of the design approach are not very demanding, software implementation would still greatly improve practical usability of the introduced new design approach.

8. REFERENCES

1. Brito, L. A. T., Dawson, A. & Kolisoja, P. (2009) Analytical evaluation of unbound granular layers in regard to permanent deformation, Proceedings of the 8th International Conference BCR2A'09, pp. 187-196
2. Chen, D.-H., Lin, ED.-F., Liau, P.-H. and Bilyeu, J. (2005). A Correlation Between Dynamic Cone Penetrometer Values and Pavement Layer Moduli, Geotechnical Testing Journal, Vol. 28, No.1, pp. 42 – 49.
3. Dawson, A. and Kolisoja, P. (2004). Permanent Deformation, Report on Task 2.1 of the ROADDEX II project, 47 p. (Available at: http://www.roadex.org/uploads/publications/docs-RII-EN/2_1%20Permanent%20Deformation_1.pdf)
4. Dawson, A., Kolisoja, P. and Vuorimies, N. (2008). Understanding Low-Volume Pavement Response to Heavy Traffic Loading, Report of the ROADDEX III project. 46 p. (Available at: http://www.roadex.org/uploads/publications/docs-RIII-EN/task-b2_designa_140408.pdf)
5. Dawson, A., Kolisoja, P., Vuorimies, N. & Saarenketo, T. (2007) Design of low-volume pavements against rutting – a simplified approach, Transportation Research Record: Journal of the Transportation Research Board. Low Volume Roads 2007, Volume 1, pp. 165 – 172.
6. Ehrola, E. (1996). Liikenneväylien rakennesuunnittelun perusteet, Rakennustieto, Helsinki. 365 p. (*In Finnish*)
7. Huang, Y. H. (1993). Pavement Analysis and Design, Prentice Hall. 805 p.
8. Kolisoja, P. (1997). Resilient Deformation Characteristics of Granular Materials, PhD Thesis, Tampere University of Technology.
9. Smoltczyk, U. (Editor)(2003), Geotechnical Engineering Handbook, Vol. 3, Elements and Structures, Ernst & Sohn
10. Ullidtz, P. (1998) Modeling Flexible Pavement Response and Performance, Polyteknisk Forlag. 205 p.

APPENDIX

APPLICATION EXAPMLES OF THE NEW MODE 2 RUTTING DESIGN APPROACH

ANALYSIS OF A BASIC DESIGN CASE

Definition of the input data for the design process

Let us assume that our design task is to decide the required aggregate layer thickness 'h' for a low volume road structure under the following presumptions (Figure A1.1):

- The design wheel load to be applied is $W = 50$ kN both for a single wheel and a pair of dual wheels
- The available aggregate can be classified as medium quality (fines content from 5 to 12 % and dielectric value from 9 to 16) and considered to be properly compacted and drained thus having a friction angle of $\varphi' = 45^\circ$ and a cohesion of $c' = 10$ kPa (Table 6.3)
- The undrained shear strength of the subgrade soil is $s_u = 15$ kPa
- The desired minimum factor of safety against total failure of the structure is $F_s = 1.8$

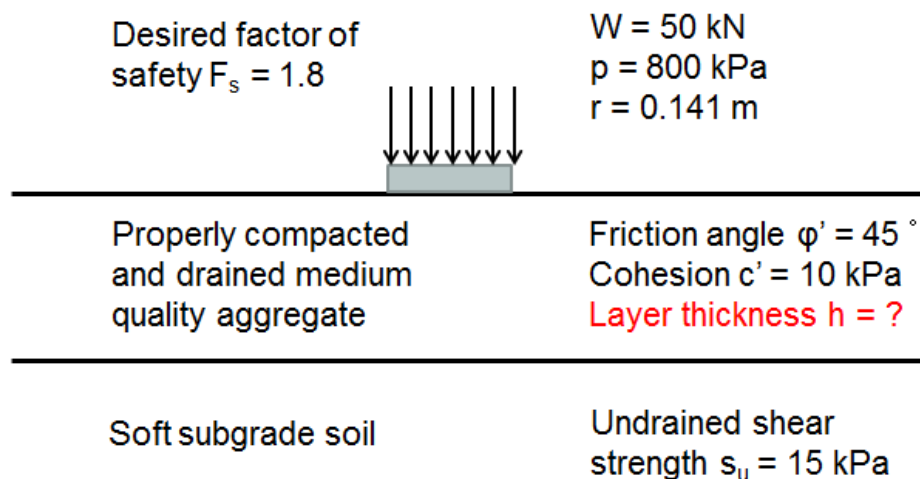


Figure A1.1 Input data for the basic design case (single wheel loading configuration).

According to the principles presented in Chapter 5.5.6 we need to choose an initial (guess) value for the layer thickness h , say 0.5 m.

Then we also need to transform the aggregate shear strength parameters φ' and c' as a value of $s_{\text{aggregate}}$ using Equation 5.2:

$$s_{\text{aggregate}} = c' + 250 \tan \varphi' = 10 + 250 \tan 45^\circ = 260 \text{ kPa}$$

Determination of the load distribution factor LDF

Using Equations 5.3 and 5.4 we get the initial value of load distribution factor LDF for the single wheel configuration as follows:

$$LDF_{initial}^{SW} = A_1 \cdot \frac{s_{agregate} - 100}{1000} + 0.20 = 4.8206 \cdot \frac{260 - 100}{1000} + 0.20 = 0.9713$$

where

$$\begin{aligned} A_1 &= 0.00785 \cdot (s_{u \text{ subgrade}})^2 - 0.37132 \cdot s_{u \text{ subgrade}} + 8.62417 \\ &= 0.00785 \cdot (15)^2 - 0.37132 \cdot 15 + 8.62417 = 4.8206 \end{aligned}$$

Similarly, using Equations 5.3 and 5.5 we get the initial value of load distribution factor LDF for the dual wheel configuration:

$$LDF_{initial}^{DW} = A_2 \cdot \frac{s_{agregate} - 100}{1000} + 0.20 = 3.9896 \cdot \frac{260 - 100}{1000} + 0.20 = 0.8383$$

where

$$\begin{aligned} A_2 &= 0.00148 \cdot (s_{u \text{ subgrade}})^2 - 0.14166 \cdot s_{u \text{ subgrade}} + 5.78148 \\ &= 0.00148 \cdot (15)^2 - 0.14166 \cdot 15 + 5.78148 = 3.9896 \end{aligned}$$

By substituting the selected initial value of $h = 0.5$ in Equation 5.6 we get the correction increment ΔLDF for the load distribution factor:

$$\begin{aligned} \Delta LDF &= 2.0652 \cdot (h - 0.4)^2 - 0.8771 \cdot (h - 0.4) \\ &= 2.0652 \cdot (0.5 - 0.4)^2 - 0.8771 \cdot (0.5 - 0.4) = -0.0671 \end{aligned}$$

After that we can determine the design values of LDF both for the single wheel and dual wheel configurations using Equation 5.7.

$$LDF_{design}^{SW} = LDF_{initial}^{SW} + \Delta LDF = 0.9713 - 0.0671 = 0.9042$$

$$LDF_{design}^{DW} = LDF_{initial}^{DW} + \Delta LDF = 0.8383 - 0.0671 = 0.7712$$

Determination of the maximum allowable wheel load

Finally we can determine the maximum allowable wheel loads corresponding to the factor of safety $F_s = 1.8$ using Equations 5.8 and 5.9.

$$W_{\max SW} = \frac{19.38}{F_s} \cdot (0.141 + h \cdot LDF_{SW})^2 \cdot s_u = \frac{19.38}{1.8} \cdot (0.141 + 0.5 \cdot 0.9042)^2 \cdot 15 = \mathbf{56.8 \text{ kN}}$$

$$W_{\max DW} = 2 \cdot \frac{19.38}{F_s} \cdot (0.100 + h \cdot LDF_{DW})^2 \cdot s_u = 2 \cdot \frac{19.38}{1.8} \cdot (0.100 + 0.5 \cdot 0.7712)^2 \cdot 15 = \mathbf{76.2 \text{ kN}}$$

Optimization of the design solutions

As the maximum allowable values for the wheel load W are now higher than the design value 50 kN we can consider of reducing the aggregate layer thickness. By repeating the same procedure as above – most practically with the aid of a spreadsheet program or some other respective software tool – we can optimize the design in the layer thicknesses indicated in Table A1.1.

Table A1.1 Summary of the optimization results for the basic design case.

	<i>Initial design</i>	<i>Optimized design</i>
W_{design} (kN)	50	50
F_s	1.8	1.8
c' (kPa)	10	10
ϕ' (°)	45	45
s_u (kPa)	15	15
h_{SW} (m)	0.5	0.45
h_{DW} (m)	0.5	0.33
$W_{\text{max_SW}}$ (kN)	56.8	50.8
$W_{\text{max_DW}}$ (kN)	76.2	51.7

In Table A1.1 we can see that according to the suggested design approach it is possible to reduce the aggregate layer thickness to 0.45 m for the single wheel loading configuration and to 0.33 m for the dual wheel loading configuration. The difference between the wheel configurations is of course due to the more efficient load spreading achieved by the dual wheel system.

These optimized layer thicknesses of 0.45 m and 0.33 m respectively can now be used in sensitivity analyses for the effects of different input parameters of the design as presented on the following pages.

For ease of comparison between the different calculation cases the numerical values related to the optimized basic calculation cases are outlined in red.

EFFECT OF AGGREGATE QUALITY

Let us first analyze how the aggregate quality affects the design. To do this we consider changing the medium quality aggregate to a good quality one. If we again assume the aggregate to be properly compacted and drained, the values of shear strength parameters suggested by Table 6.3 are now $\phi' = 50^\circ$ and $c' = 25$ kPa.

By applying these values as input data into the design procedure and by making the optimization for layer thicknesses we get the results summarized in Table A1.2. (The values of the optimized basic calculation case is outlined in red.)

Table A1.2 Effect of improving the aggregate quality.

	Medium quality aggregate	Good quality aggregate	
		Original layers	Optimizes layers
W_{design} (kN)	50	50	50
F_s	1.8	1.8	1.8
c' (kPa)	10	25	25
ϕ' ($^\circ$)	45	50	50
s_u (kPa)	15	15	15
h_{SW} (m)	0.45	0.45	0.31
h_{DW} (m)	0.33	0.33	0.23*
$W_{\text{max_SW}}$ (kN)	50.8	78.5	51.7
$W_{\text{max_DW}}$ (kN)	51.7	75.4	51.3

*) Layer thickness below the range covered by the performed FEM analyses.

These indicate that if the aggregate layer is made using a better quality aggregate at the same layer thicknesses, the maximum allowable wheel loads increase markedly above 70 kN (the mid column of Table A1.2). Conversely, the analysis suggests that for the original value of design wheel load 50 kN it would be possible to reduce the layer thickness down to 0.31 m for the single wheel configuration and to 0.23 m for the dual wheel configuration, i.e by 140 mm for the single wheel loading and by 100 mm for the dual wheel loading case. The latter result must, however, be treated with some caution as the layer thickness is already quite a lot lower than those included in the FEM analyses performed in this research.

Next we shall analyze the respective effect of the use of a poor aggregate quality. Assuming again proper compaction and drainage of the layer but high fines content ($> 12\%$) and high dielectric value (> 16) for the aggregate we get the suggested values of $\phi' = 40^\circ$ and $c' = 10$ kPa from Table 6.3. In fact in this case it is only the friction angle that changes in comparison to the basic design case while the cohesion remains at the same level. The design results obtained for this poor quality aggregate have been summarized in Table A1.3.

Table A1.3 Effect of lowering the aggregate quality.

	Medium quality aggregate	Poor quality aggregate	
		Original layers	Optimizes layers
W_{design} (kN)	50	50	50
F_s	1.8	1.8	1.8
c' (kPa)	10	10	10
ϕ' ($^\circ$)	45	40	40
s_u (kPa)	15	15	15
h_{SW} (m)	0.45	0.45	0.62*
h_{DW} (m)	0.33	0.33	0.48
$W_{\text{max_SW}}$ (kN)	50.8	36.2	51.6
$W_{\text{max_DW}}$ (kN)	51.7	39.0	51.2

*) Layer thickness above the range covered by the performed FEM analyses.

If the layer thicknesses were kept at the original values (the mid column of Table A1.3) the maximum allowable wheel loads would now reduce well below 40 kN. This would mean a high risk of immediate collapse of the road structure if it was exposed to the design wheel load of 50 kN. The result of lowering the aggregate quality would in this case mean an increase in the required aggregate layer thickness of about 150 mm (the rightmost column of Table A1.3). Here again it must be noted that the layer thickness of 0.62 m for the single wheel configuration exceeds the values used in the FEM analysis.

All in all it can be concluded that, according to the suggested new Mode 2 rutting design approach, the aggregate quality clearly seems to have a marked effect on the required layer thickness of a low volume road structure.

EFFECT OF AGGREGATE MOISTURE CONTENT

In the suggested values of shear strength parameters shown in Table 6.3 an increase in the moisture content of the aggregate layer is assumed to result in a lower value of cohesion c' . Because the values of cohesion suggested for the normal moisture content conditions are not very high either, the effect of higher moisture content is relatively modest (the leftmost column in Table A1.4).

As already discussed in chapter 6.4 the tabulated values of cohesion for the aggregate materials in normal moisture content do not allow for any effects of the wetting-drying cycles that happen in real road structures during a dry summer season. Therefore, the suggested values of cohesion shown should be considered fairly conservative with regard to dry summer season conditions. To demonstrate how this could affect the results of Mode 2 rutting analysis a higher assumption of $c' = 50$ kPa was also made and shown below (the rightmost column in Table A1.4).

Table A1.4 Summary of the effect of aggregate moisture content.

	<i>High moisture content</i>	<i>Normal moisture content</i>	<i>Dry season moisture content</i>
W_{design} (kN)	50	50	50
F_s	1.8	1.8	1.8
c' (kPa)	5	10	50
ϕ' (°)	45	45	45
s_u (kPa)	15	15	15
h_{SW} (m)	0.47	0.45	0.35
h_{DW} (m)	0.34	0.33	0.26
$W_{\text{max_SW}}$ (kN)	51.0	50.8	51.7
$W_{\text{max_DW}}$ (kN)	51.3	51.7	52.2

In Table A1.4 we can observe that the differences in the required aggregate layer thicknesses between the normal moisture content and high moisture content are very small for the reason already discussed above. Meanwhile, if the material is in a dry condition, the required minimum layer thickness may be about 100 mm lower than at the normal moisture content.

One very important remark that should be made here is that the small difference between the normal and high moisture content conditions should by no means be interpreted that proper drainage of a low volume road structure would not be of utmost importance concerning its performance under heavy wheel loads. In the present case we must acknowledge that the FEM analyses undertaken correspond to one-time slow load application only and the very important accumulating effect of repeated loading in wet conditions is therefore not covered by the results presented above.

EFFECT OF SUBGRADE QUALITY

This analysis will examine the effect of subgrade quality on the required layer thicknesses under a design wheel load of 50 kN. In the results summarized in Table A1.5 the undrained shear strength of the subgrade soil is varied from 10 to 20 kPa while the aggregate is again assumed to be of medium quality and the aggregate layer is assumed to be properly compacted and drained.

Table A1.5 Summary of the effect of subgrade quality.

	<i>Very soft subgrade</i>	<i>Soft subgrade</i>	<i>Medium soft subgrade</i>
W_{design} (kN)	50	50	50
F_s	1.8	1.8	1.8
c' (kPa)	10	10	10
ϕ' (°)	45	45	45
s_u (kPa)	10	15	20
h_{SW} (m)	0.53	0.45	0.38
h_{DW} (m)	0.43	0.33	0.27
$W_{\text{max_SW}}$ (kN)	51.0	50.8	51.2
$W_{\text{max_DW}}$ (kN)	50.8	51.7	51.9

The results show in Table A1.5 indicate clearly that the subgrade quality has a marked effect on the required aggregate layer thickness as can of course be expected in the case of Mode 2 subgrade rutting. On the analysed range of layer thicknesses an increase of 5 kPa in the undrained shear strength of the subgrade soil enables reduction of the aggregate layer thickness by almost 100 mm, a fact that clearly underlines the importance of sufficiently thorough soil investigations when building or renovating low volume roads located on soft subgrade areas.

EFFECTS OF LOWERING THE DESIGN REQUIREMENTS CONCERNING WHEEL LOAD AND/OR FACTOR OF SAFETY

As in the last application example this analysis will investigate the effects of lowering the design wheel load – i.e. the effect of applying a weight restriction – and the required factor of safety against failure. The later might be considered as an applicable approach on some occasions if the number of load repetitions is going the very low, and the consequences of a possible failure of the road structure are not very severe.

In the analysis the material parameters of the aggregate layer are selected to correspond a properly compacted poor quality aggregate in high moisture content. The applied values for friction angle and cohesion are thus $\varphi' = 40^\circ$ and $c' = 10$ kPa respectively (Table 6.3). The undrained shear strength of the subgrade soil is again assumed to be 15 kPa.

At first the required aggregate layer thicknesses are determined for the design wheel load of 50 kN and the safety factor of 1.8 (the leftmost column in Table A1.6). After that only the required factor of safety is lowered to 1.5, and then only the design wheel load is lowered to 30 kN (results in the two mid columns of Table A1.6). Finally the combined effects of lowering both the wheel load to 30 kN and the safety factor to 1.5 is analysed in the rightmost column of Table A1.6.

Table A1.6 Effects of lowering the design wheel load and/or safety factor.

	Nominal design requirements	Lowered safety factor S_f	Lowered design wheel load W	Both W and S_f lowered
W_{design} (kN)	50	50	30	30
F_s	1.8	1.5	1.8	1.5
c' (kPa)	0	0	0	0
φ' ($^\circ$)	40	40	40	40
s_u (kPa)	15	15	15	15
h_{SW} (m)	0.66*	0.59*	0.41	0.32
h_{DW} (m)	0.54	0.43	0.27	0.21*
$W_{\text{max_SW}}$ (kN)	51.3	51.8	30.8	31.2
$W_{\text{max_DW}}$ (kN)	51.7	51.3	31.5	31.4

*) Layer thickness beyond the range covered by the performed FEM analyses.

For the nominal design requirements of wheel load and factor of safety the analysis in this case results in the layer thicknesses clearly exceeding half a metre. Lowering the factor of safety alone enables the aggregate layer thickness to be reduced by about 100 mm. Lowering the allowed wheel load alone enables a reduction in the aggregate layer thickness by about 250 mm in comparison to the structure needed for the nominal design requirements.

Some further reduction of the required aggregate layer thicknesses can be achieved by lowering both the design wheel load and the safety factor even though, especially in the case of dual wheel configuration, the analysis results are again ending up on layer thicknesses clearly beyond the range covered by the FEM analyses performed. In any case, the analysis is in good agreement with the practical experience that in extreme loading conditions the application of a weight restriction is an efficient way of preventing a low volume road from being destroyed by heavy wheel load applications.

ROADEX PROJECT REPORTS (1998–2012)

This report is one of a suite of reports and case studies on the management of low volume roads produced by the ROADEX project over the period 1998-2012. These reports cover a wide range of topics as below.

- Climate change adaptation
- Cost savings and benefits accruing to ROADEX technologies
- Dealing with bearing capacity problems on low volume roads constructed on peat
- Design and repair of roads suffering from spring thaw weakening
- Drainage guidelines
- Environmental guidelines & checklist
- Forest road policies
- Generation of 'snow smoke' behind heavy vehicles
- Health issues raised by poorly maintained road networks
- Managing drainage on low volume roads
- Managing peat related problems on low volume roads
- Managing permanent deformation in low volume roads
- Managing spring thaw weakening on low volume roads
- Monitoring low volume roads
- New survey techniques in drainage evaluation
- Permanent deformation, from theory to practice
- Risk analyses on low volume roads
- Road condition management of low volume roads
- Road friendly vehicles & tyre pressure control
- Road widening guidelines
- Socio-economic impacts of road conditions on low volume roads
- Structural innovations for low volume roads
- Treatment of moisture susceptible materials
- Tyre pressure control on timber haulage vehicles
- Understanding low volume pavement response to heavy traffic loading
- User perspectives on the road service level in ROADEX areas
- Vehicle and human vibration due to road condition
- Winter maintenance practice in the Northern Periphery

All of these reports, and others, are available for download free of charge from the ROADEX website at www.ROADEX.org.